

ASCAT-C Level 1 Commissioning Report

Doc.No. : EUM/RSP/REP/18/1035367
Issue : v1A
Date : 18 February 2019
WBS/DBS:

EUMETSAT
Eumetsat-Allee 1, D-64295 Darmstadt,
Germany
Tel: +49 6151 807-7
Fax: +49 6151 807 555
<http://www.eumetsat.int>

Page left intentionally blank

Document Change Record

<i>Version</i>	<i>DCR</i>	<i>Description of Changes</i>
V1	n/a	First issue

Table of Contents

1	INTRODUCTION	6
1.1	Purpose	6
1.2	Scope	6
1.3	Description of Validation Environment	6
1.4	Applicable Documents	7
1.5	Reference Documents	7
1.6	List of acronyms and abbreviations	7
1.7	Document Structure	8
2	CALIBRATION AND VALIDATION BY EUMETSAT	9
2.1	Internal calibration – locking of calibration constants	9
2.2	Monitoring of instrument telemetry	10
2.3	Monitoring of reference functions	12
2.3.1	Power-gain product (PGP)	12
2.3.2	Noise power (NP)	13
2.3.3	Receive filter shape (Hrx)	15
2.4	Gain compression monitoring	15
2.5	Initial cross-calibration with ASCAT-A and B	16
2.6	Level 1B product: monitoring of swath geometry	17
2.7	External calibration	19
2.7.1	Antenna mispointing angles	20
2.8	Improved cross-calibration	21
2.9	Validation using natural targets	22
2.9.1	Amazon rainforest	22
2.9.2	Open ocean	24
2.9.3	Antarctic ice	26
2.9.4	Global backscatter	27
2.10	Accuracy of the nominal backscatter (Kp)	28
2.11	Flag validation	29
3	VALIDATION BY EXTERNAL PARTNERS	31
3.1	OSI-SAF (KNMI)	31
3.2	H-SAF (TU-Wien)	32
4	SUMMARY AND CONCLUSIONS	34
APPENDIX A	GROUND SEGMENT CONFIGURATION CHANGES	35
APPENDIX B	INSTRUMENT TELEMETRY	36

ASCAT-C Level 1 Commissioning Report

B.1	Temperatures	36
B.2	Equipment voltages.....	37
B.3	Equipment powers	38
B.4	Equipment temperatures.....	40
B.5	ADC Voltages, gain and offsets	41

1 INTRODUCTION

1.1 Purpose

This report describes the calibration and validation of the data from the Advanced SCATterometer (ASCAT) on the EUMETSAT Polar System (EPS) Metop-C satellite performed as part of the satellite and instrument commissioning.

The Metop-C satellite was launched from Kourou on 2018-11-07. ASCAT-C was switched on for the first time on 2018-11-13. The satellite commissioning and cal/val testing aims at verifying the capability of the satellite and ground segment to provide operational services with the required levels of availability, timeliness and quality. In particular, the main objective of cal/val is to ensure that the quality of the products satisfies the operational requirements.

1.2 Scope

This report is submitted to the product validation review board in order to decide on the readiness for operational dissemination of the above list of products. It is intended for the members of the Science and Products Validation Team (SPVT), as well as to the Metop-C commissioning management. It is also intended to publish this report and make it available to all ASCAT users via the EUMETSAT web site.

Previous issues of this document have assessed the readiness to distribute products to cal/val partners, as well as to all users with a pre-operational status. We would like to thank the following groups, who have provided feedback and helped us improving the Metop-C Level 1 service:

- The Ocean and Sea ice Satellite Applications Facility (OSI-SAF)
- The Satellite Applications Facility on support to Operational Hydrology and Water Management (H-SAF)
- The European Centre for Medium Range Weather Forecasting (ECMWF)
- The Met Office

1.3 Description of Validation Environment

The product validation has been performed with the following elements:

- EPS validation ground segment (GS1 and GS2) running ASCAT Product Processing Facility (PPF) 10.3.0
- Technical Computing Environment (TCE) off-line ASCAT PPF v10.3.0
- TCE Data Processing Software (DPS), daily reports and off-line validation tools
- EPS Product Quality Monitoring validation environment (EPQM VAL) and daily reports
- CHART telemetry monitoring system

1.4 **Applicable Documents**

AD-1	ASCAT Verification, Calibration and Validation Plan	EUM/RSP/DOC/17/897474
AD-2	EPS Cal/Val Overall Plan	EUM.EPS.SYS.PLN.02.004

1.5 **Reference Documents**

RD-1	ASCAT Instrument Operations Manual (IOM)	MO-MA-DOR-SC-0008
RD-2	Estimation of ASCAT-Normalised Radar Cross Section: ATBD	EUM/TSS/SPE/14/762689

1.6 **List of acronyms and abbreviations**

ASCAT-A	Advanced SCATterometer on METOP-A (M02)
ASCAT-B	Advanced SCATterometer on METOP-B (M01)
ASCAT-C	Advanced SCATterometer on METOP-C (M03)
CAL	Calibration
Cal/Val	Calibration and Validation
DPS	Data Processing System (for product quality monitoring)
ECMWF	European Centre for Medium Range Weather Forecasting
EPQM OPE/VAL	EPS Product Quality Monitoring OPERational and VALidation environments
EPS	European Polar System
EUMETSAT	European Organisation for the Exploitation of Meteorological Satellites
GCM	Gain Compression Monitoring
GS1	Operational Ground Segment
GS2	Validation Ground Segment
GS3	Integration Ground Segment
HKTM	House Keeping TeleMetry
Hrx	Receive Filter Shape
H-SAF	Satellite Applications Facility on support to Hydrology and Water Management
ISP	Instrument Source Packet
METOP	METEorological Operational Platform
NOAA	National Atmospheric and Oceanic Administration
NOC	NWP Ocean Calibration
NWP	Numerical Weather Prediction
NP	Noise Power
NTG	Normalisation Table Generation
OSI-SAF	Ocean and Sea Ice Satellite Applications Facility

PDU	Processing Data Unit
PGP	Power Gain Product
PPF	Product Processing Facility
SIOV	System In Orbit Verification
SPVT	Science and Products Validation Team
SWET	Software Engineering Task
TCE	Technical Computing Environment
WVC	Wind Vector Cell

1.7 Document Structure

- Section 1 General information (this section)
- Section 2 Internal EUMETSAT product validation
- Section 3 Product validation by external partners
- Section 4 Conclusions
- Section 5 Recommendations

2 CALIBRATION AND VALIDATION BY EUMETSAT

The tasks identified in AD-1 for ASCAT-C product commissioning are:

1. Internal calibration – locking of calibration constants
2. Initial calibration – verification and refinement
3. Level 1a product – monitoring of instrument telemetry
4. Level 1a product – reference function monitoring
5. Gain compression monitoring
6. External calibration – gain pattern generation
7. External calibration – geolocation accuracy assessment
8. External calibration – monitor ASCAT pulse shape
9. Level 1b product – monitoring of swath geometry
10. Level 1b product – validation using rainforests
11. Level 1b product – validation using ocean
12. Level 1b product – validation using sea ice
13. Level 1b product – quality flags assessment
14. Tuning and modification of product generation
15. Overall assessment and reporting.

In the following sections we will report on the activities and results associated to each task.

Note that the validation results given here are based on data generated in GS2/1 or the TCE with the ASCAT PPF v10.3.

2.1 Internal calibration – locking of calibration constants

Six parameters (usually called the ‘ccal’ parameters) are specified in the AUX_PRC data file and are used to scale the internal calibration measurements and bring them to the correct level for use in processing. At launch, the parameters were set to a first-guess value of $7.5e-9$.

The values are then modified so that the power-gain product (calculated from the ASCAT internal calibration data) in each of the six beams at a target time and position has a value of 1. To do this, we select three consecutive PDUs from orbit #365 which passes over the transponder sites in ascending direction, and does not have a scheduled calibration pass (and hence no gaps in the data). The files are:

- ASCA_XXX_00_M03_20181202183000Z_20181202183300Z_N_C_20181202191720Z
- ASCA_XXX_00_M03_20181202183300Z_20181202183600Z_N_C_20181202191833Z
- ASCA_XXX_00_M03_20181202183600Z_20181202183900Z_N_C_20181202191944Z

They are processed on the TCE using a standalone PPF installation (v10.3), and static aux files tagged as PPF_ASCAT_AUX_DU-19.0.0-1 in the svn repository. The cCal values in the input PRC file are adjusted to set the power gain product to 1 in the output Level 1a file at the target position (T1 transponder site).

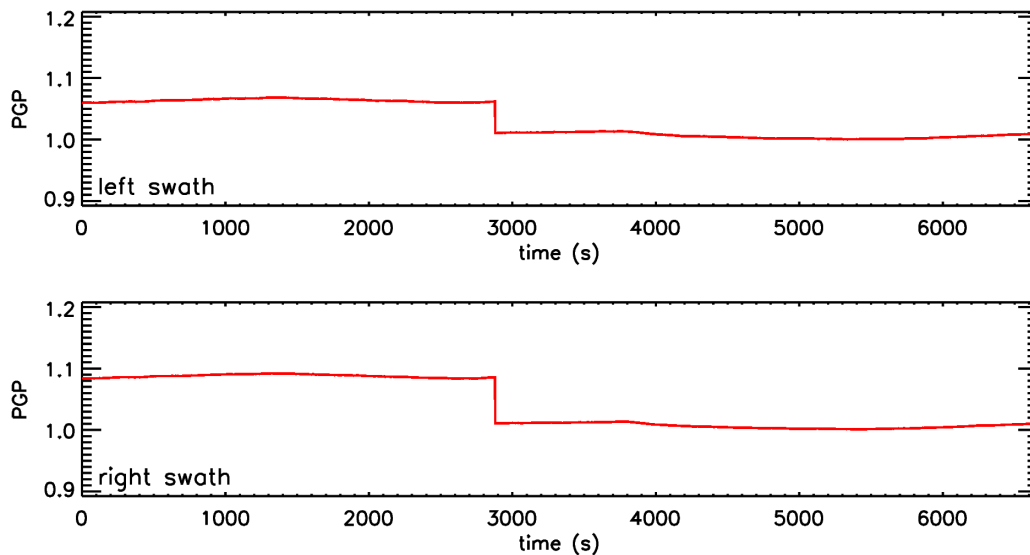
The new ccal values are $7.0588235e-09$, $7.1367399e-09$, $7.1585377e-09$, $7.0588235e-09$, $6.9838905e-09$ and $7.0688030e-09$.

The L0 files are reprocessed with the updated values and we confirm that the PGP at the selected points is equal to 1:

Table 1: Ccal locking

Beam	Distance to T1 (km)	Latitude (deg)	Longitude (deg)	Power gain product	cCal
0	324.6	39.625718	29.027277	1.0000000	7.0588235e-09
1	409.3	39.604086	28.040946	1.0000000	7.1367399e-09
2	345.8	39.597673	28.780803	1.0000000	7.1585377e-09
3	878.5	39.607734	43.050305	1.0000000	7.0588235e-09
4	964.4	39.585741	44.054133	1.0000000	6.9838905e-09
5	899.5	39.604369	43.295746	1.0000000	7.0688030e-09

The updated AUX_PRC (svn tag PPF_ASCAT_AUX_DU-20.0.0) file was installed on GS2 and GS1 on 2018-12-13. The transition to the new power gain values at the time of the auxiliary file update can be seen in Figure 1.


Figure 1: Level-1a power gain product time series, mid beams, 2018-12-12 09:00:00 UTC – 10:50:59 UTC

2.2 Monitoring of instrument telemetry

The integrated transmit power for the right mid (RM) antenna (BND0183) is higher than the values measured at the other antennas. The transmitted power detector diode shows a higher power level when the RM Antenna is transmitting (Figure 2); this is only seen with Sequencer Table 8 and is not seen with Table 1 (the sequencer tables are part of the instrument configuration and control the instrument timing and signal paths). It is possible that it is caused by a power reflection from the RM antenna flange going around the ring of circulators back to the TX coupler and towards the power detector diode. This behaviour is documented in EUM/EPs/AR/18439.

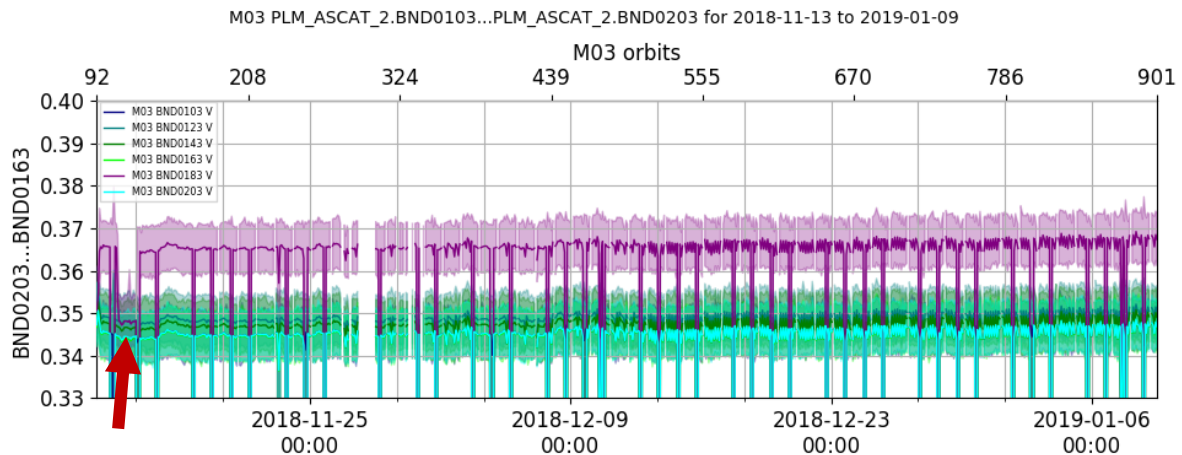


Figure 2: Integrated transmit powers 1-6 corresponding to beams 0 to 5. The period where Table 1 was used is indicated by the arrow.

During earlier activities of the ASCAT SIOV on the Metop-C spacecraft, unusually high reflected power values were initially seen in the right aft (RA) antenna (BND0205) when using measurement Table 8. Figure 3 shows that the RA antenna appears to have a higher level of integrated calibrated powers than the other antennas. According to the instrument manufacturer, this effect might be related to temperature. It is documented by EUM/EPS/AR/18355.

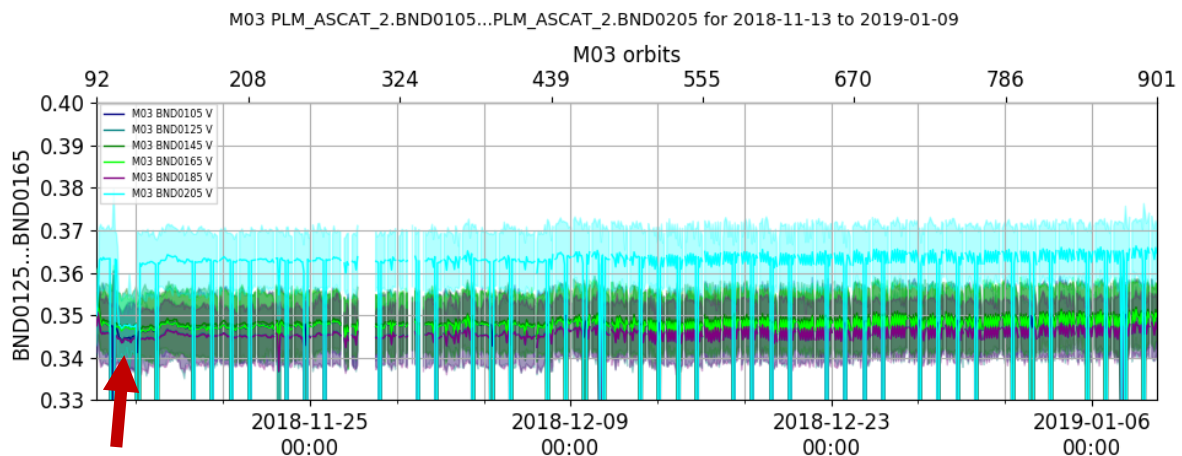


Figure 3: Integrated cal powers 1-6 corresponding to beams 0 to 5. The period where Table 1 was used is indicated by the arrow.

Both issues are considered “out of family”, but are within the specifications. They will be subject to further analysis and discussion with the instrument manufacturer. No significant impact on the products is expected.

Time series of additional instrument telemetry parameters from the house keeping telemetry (HKTM) packets are included in Appendix B. Those time series reveal that all telemetry is within the expected thresholds, as specified in the ASCA_PRC_xx_M03 file for near real time Level 1a product flagging.

2.3 Monitoring of reference functions

2.3.1 Power-gain product (PGP)

Figure 4 shows the power gain product for all beams from 2018-11-13. We observe an increase over the initial period, which can be related to instrument temperature. The drop in the PGP on 2018-12-13 is caused by the internal calibration locking (Section 1). After that, the PGP shows a slightly increasing trend which has stabilised by the end of January 2019. The effect of EUM/EPS/AR/18439 (apparently high integrated transmit power) on the PGP can be observed when the measurement mode 1 was used for a short period of time during SIOV.

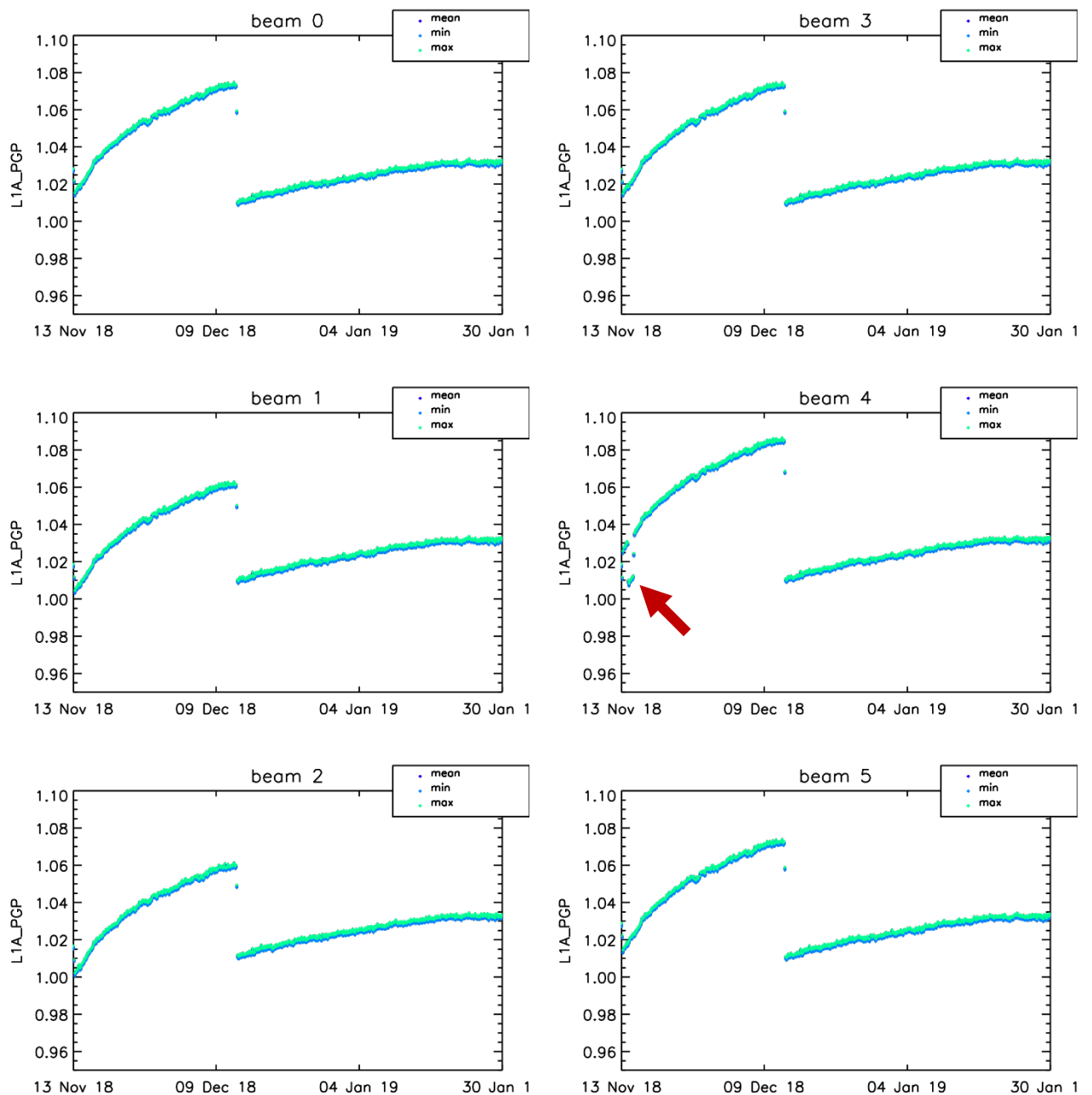


Figure 4: Power gain product from L1A data (3-hour averages). The period where Measurement Table 1 was used is indicated by the arrow. Data from GS1.

2.3.2 Noise power (NP)

Figure 5 shows time series of NP since 2018-11-13. For both ASCAT-A and B, noise values above an empirically determined threshold of 900 (in counts) were considered to be outliers. Compared to ASCAT-A and -B, the noise power for ASCAT-C seems to be slightly higher.

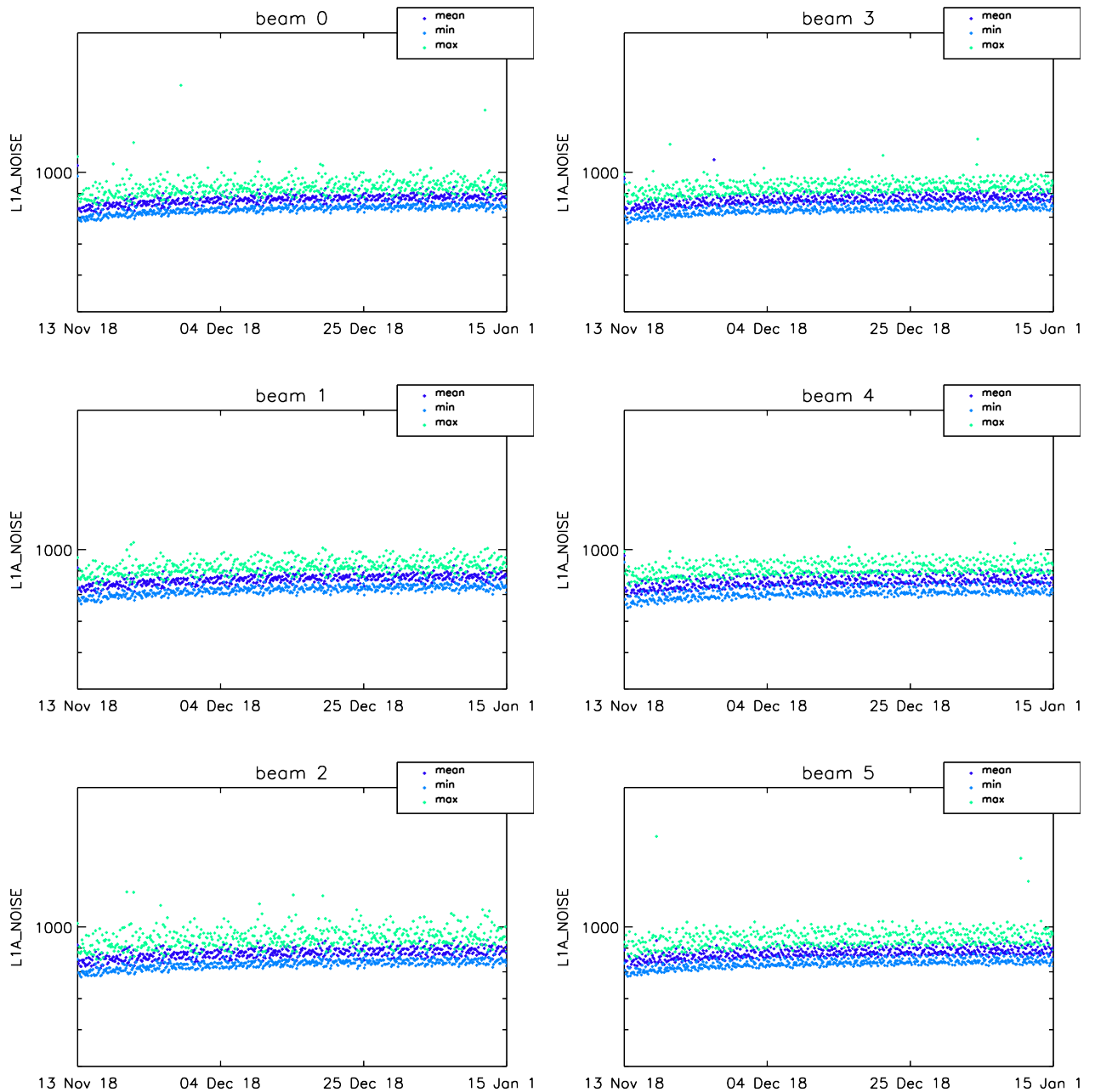


Figure 5: Noise power time series in counts for all beams, from the Level 1A products (3-hour averages). Data from GS1.

To investigate this behaviour, one month of Level-1A data over the rainforest validation site (70.0°W - 60.5°W, 5.0°S - 2.5°N) was analysed for all three ASCAT instruments. The time period for this analysis ranges from 2018-12-24 to 2019-01-23, and the data was copied from the GS1 rolling archive. We computed the signal-to-noise ratio (SNR) for the data at each 1° incidence angle bin, correcting for filter shape.

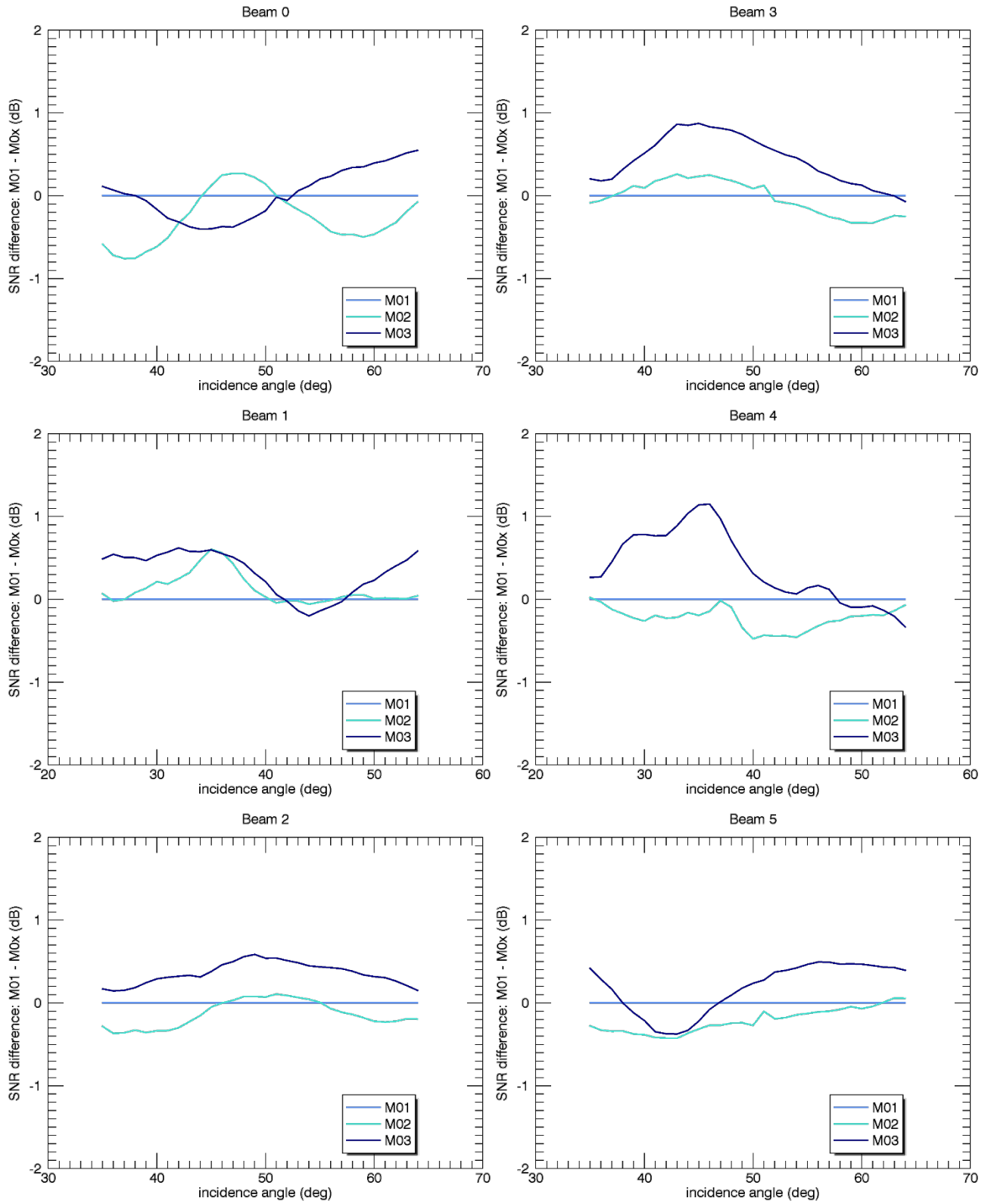
ASCAT-C Level 1 Commissioning Report


Figure 6: SNR differences with respect to ASCAT-B. Positive values indicate lower SNR.

Figure 6 shows the SNR difference with respect to ASCAT-B. We can confirm that the SNR seems to be slightly lower than for ASCAT-A and -B, by up to 1dB. This is within the value range we see for the difference between ASCAT-A and -B.

2.3.3 Receive filter shape (Hrx)

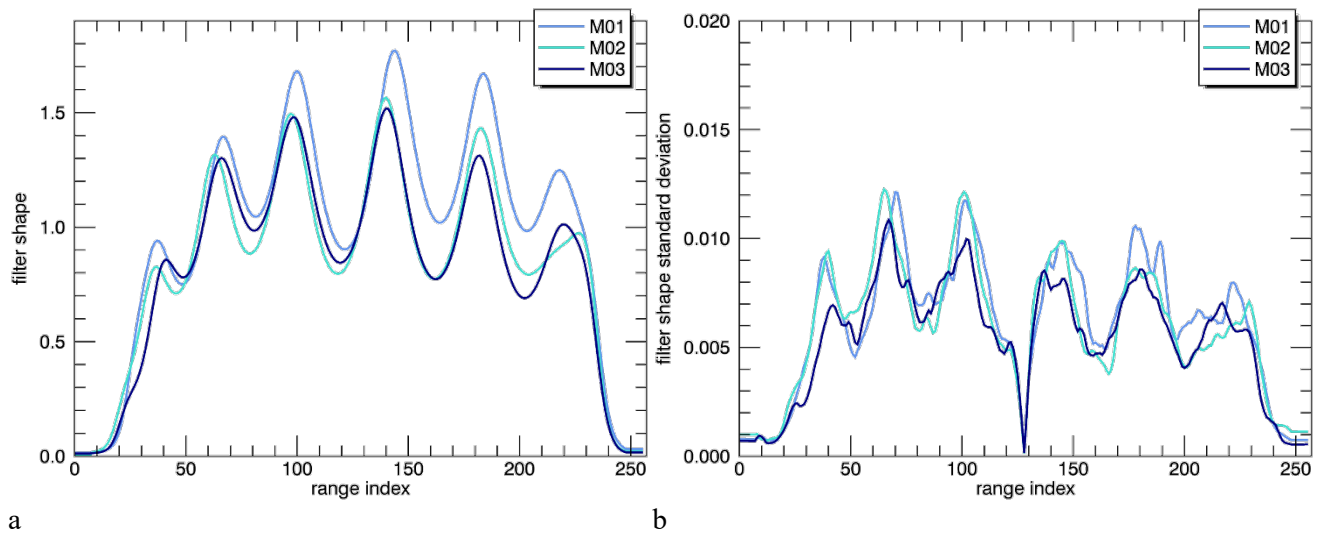


Figure 7: a) mean hrx, b) hrx standard deviation

Figure 7 shows the mean filter shape for ASCAT-A, B and C for the rainforest calibration region, averaged over the time period from 2018-12-24 to 2019-01-23. The ASCAT-C filter shape shows similar properties as the filter shapes for ASCAT-A and B, and no outliers were observed in the daily monitoring (Figure 8).

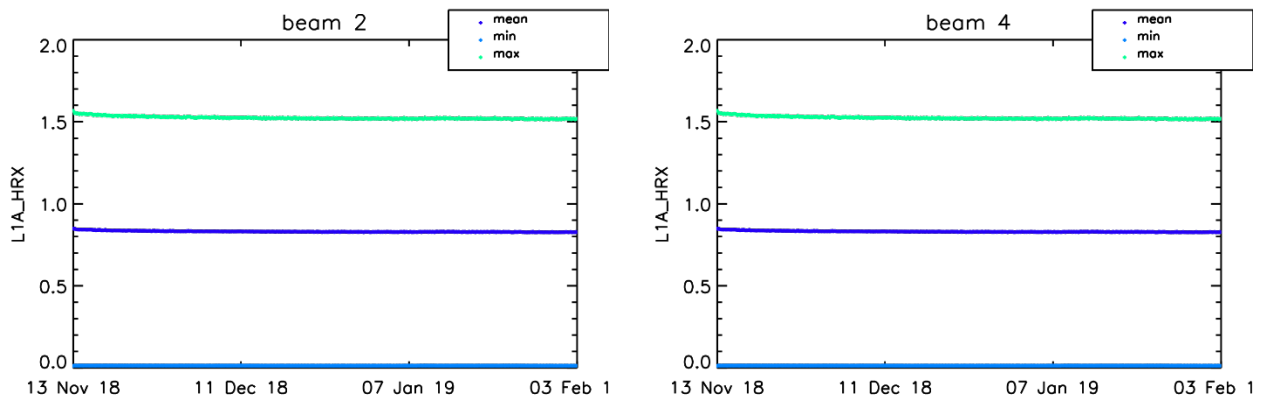


Figure 8: hrx time series for the mid beams, from 2018-11-13 onward (3-hour averages). Data from GS1.

2.4 Gain compression monitoring

The ASCAT gain compression monitoring (GCM) procedure cycles through various settings of the on board gain and is intended to check that the operational gain setting is appropriate and that the instrument is behaving linearly. GCM is performed approximately monthly. The first two GCM for ASCAT-C were performed in quick succession during early SIOV and within Svalbard visibility. The expected GCM files were generated in GS2 and further analysed off-line. The key check parameters derived from the GCM measurements according to the algorithms specified by the instrument manufacturer are shown the figure below (together with the results from two subsequent GCM procedures approximately 4 weeks and 8 weeks later) and are seen to be stable and within limits.

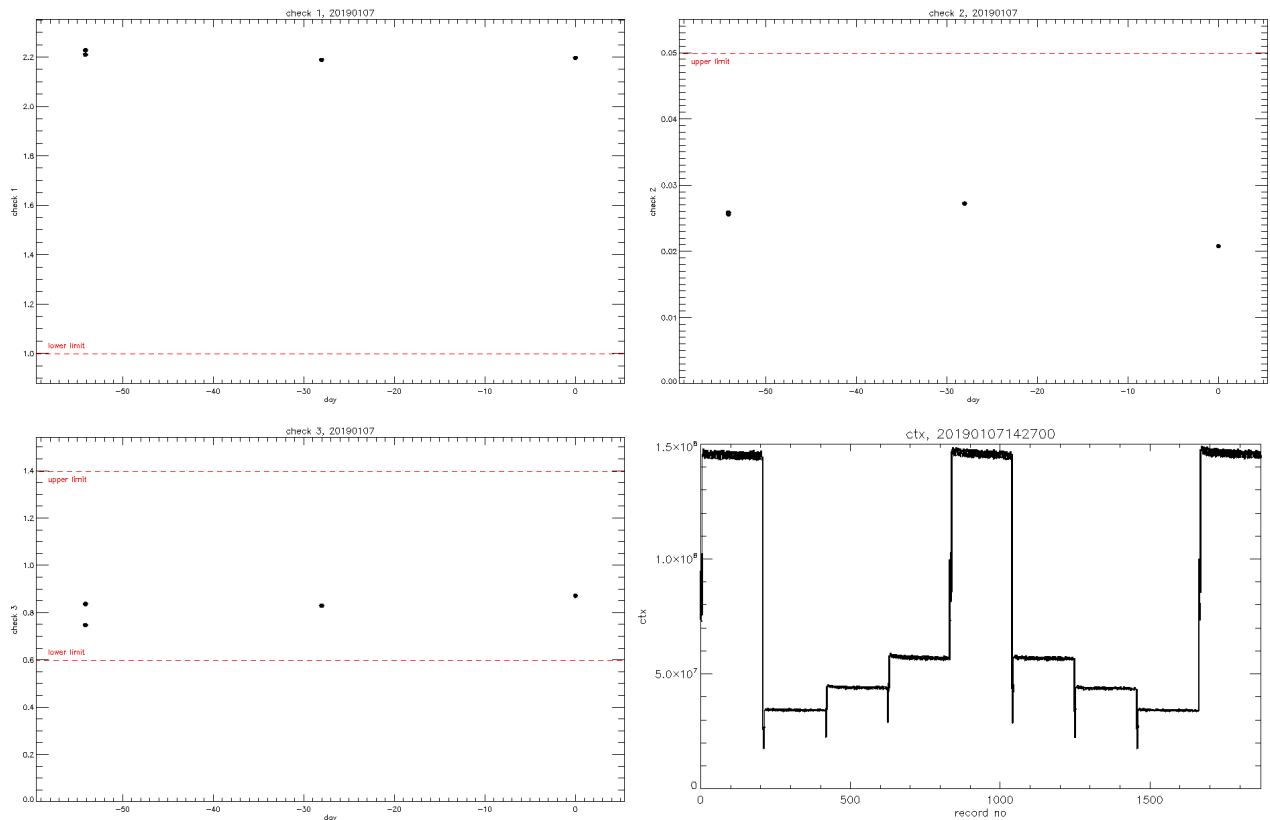


Figure 9: Time series of the Gain Compression checks for ASCAT-C

These results demonstrate that the on board gain setting is appropriate for operational use and that the instrument is behaving normally.

2.5 Initial cross-calibration with ASCAT-A and B

The ASCAT instruments are calibrated using the signals provided by a number of ground based transponders. Several months of transponder needs to be collected to allow an accurate calibration. While the data is being collected we cross-calibrate ASCAT-C with ASCAT-A and B in order to obtain usable products as soon as possible. ASCAT-A and B were last calibrated in 2015 but both instruments have been continuously monitored and are known to be very stable, and so they can be regarded as correctly calibrated.

To perform the cross-calibration we collect 25 days (2018-12-14 to 2019-01-07) of ASCAT-A, B and C data over the Amazon rainforest. We calculated the parameter $\gamma_0 = \sigma_0 / \cos \theta$, where σ_0 is the normalised radar cross section and θ is the incidence angle. The ASCAT-A and B γ_0 was averaged together and the ASCAT-C gain pattern was modified so that the ASCAT-C backscatter values produced from the processor matched the averaged A and B data as much as possible. The results are shown in the figures below and seem good for the mid and aft beams (with differences below 0.1 dB) but relatively poor in the fore beams (with differences of over 0.2 dB). For an initial calibration intended to last for a few weeks while transponder data was collected, this was regarded as acceptable.

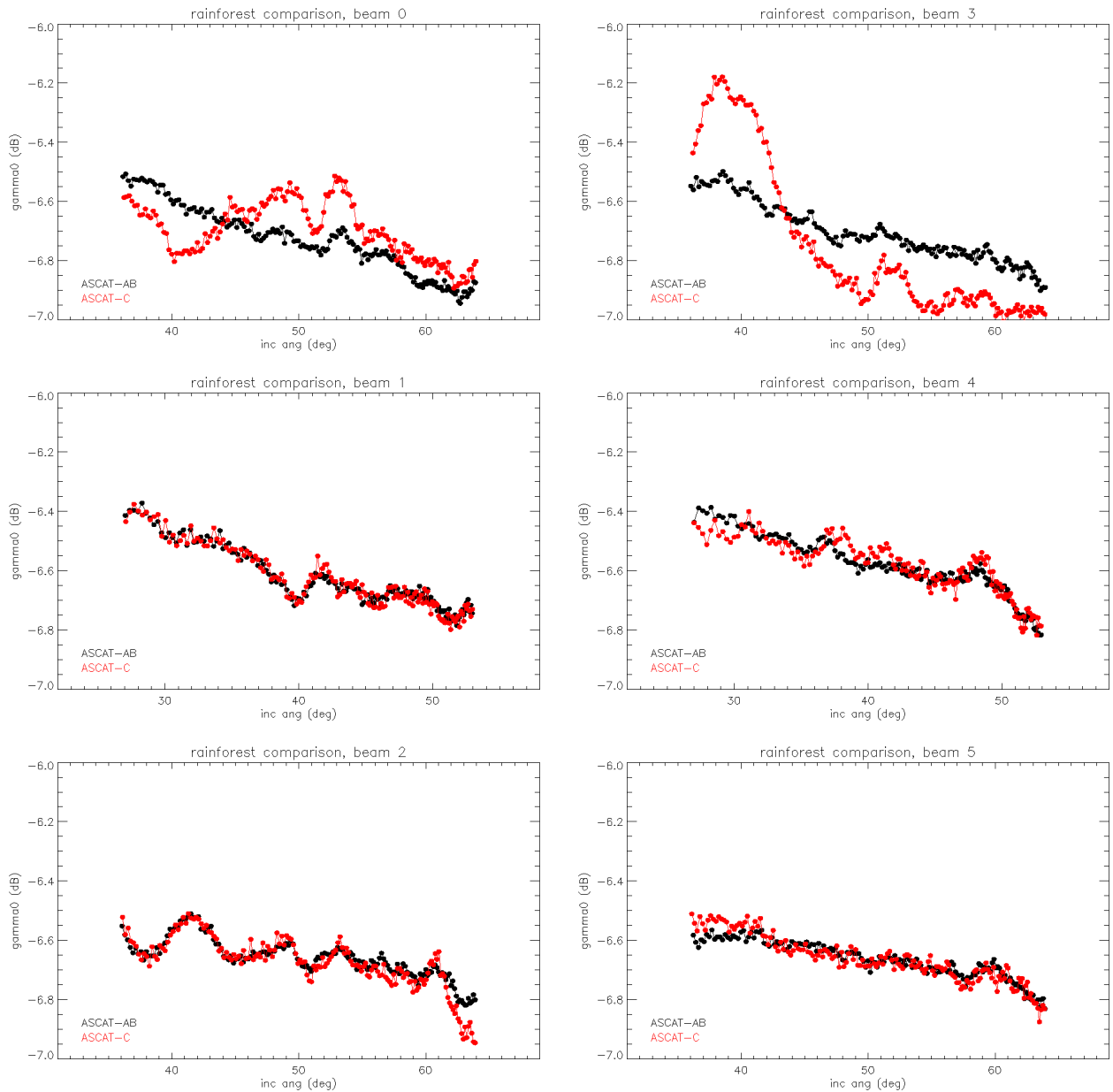
ASCAT-C Level 1 Commissioning Report


Figure 10: γ_0 patterns over the rainforest from given by the cross calibration of ASCAT-C with ASCAT-A/B.

This calibration became active in GS2 on 2019-01-16 and in GS1 on 2018-01-22. A complete list of the calibration updates during cal/val is given in Appendix A.

2.6 Level 1B product: monitoring of swath geometry

The swath geometry can be verified by checking that the incidence and azimuth angle values in the level 1B are within the expected ranges. Figure 11 and Figure 12 show those values for ASCAT-C. They behave as expected and are very similar to ASCAT-A and B.

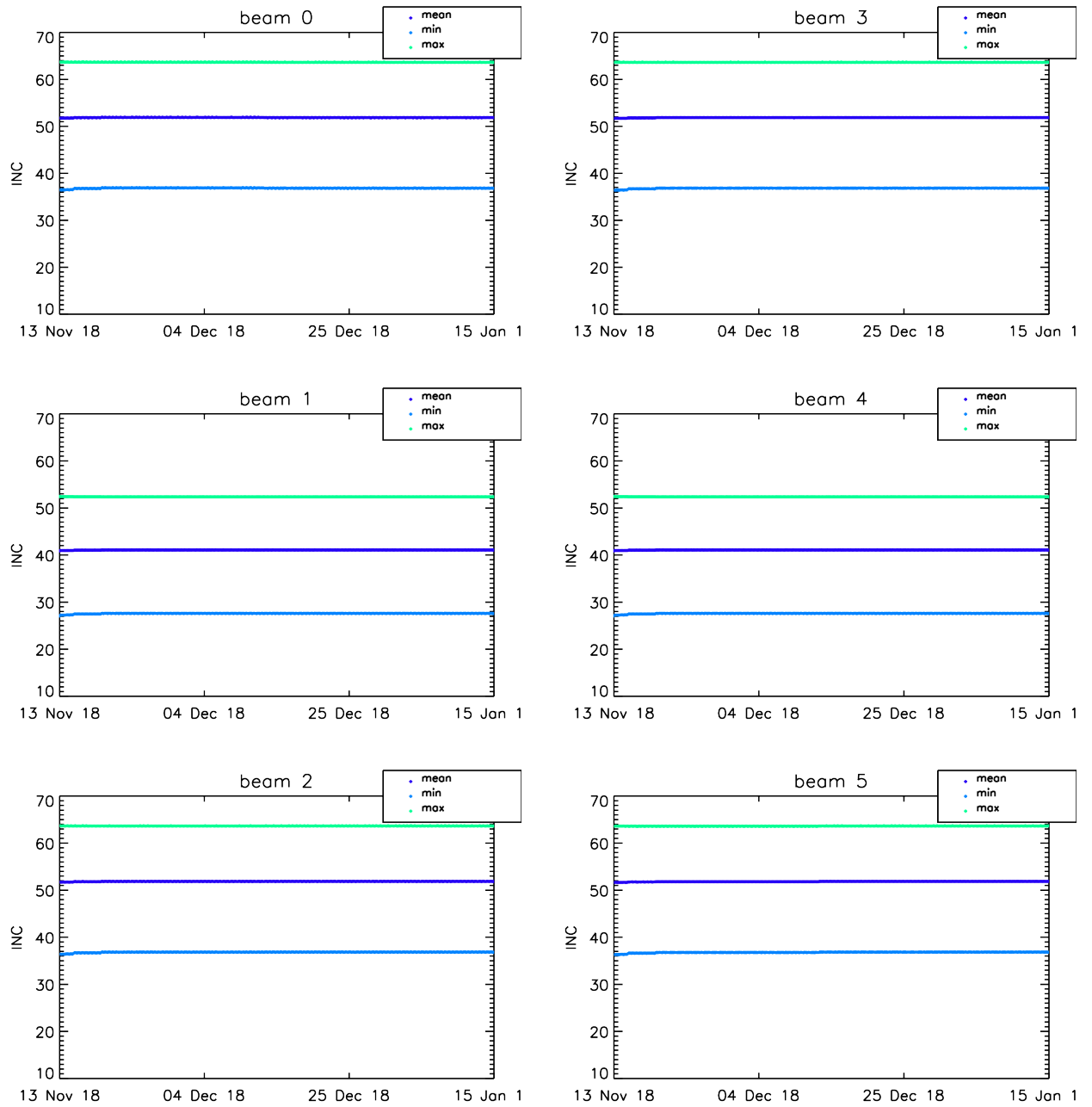
ASCAT-C Level 1 Commissioning Report


Figure 11. Incidence angles (in degrees). The plots show three-hour average values. Data from GS1.

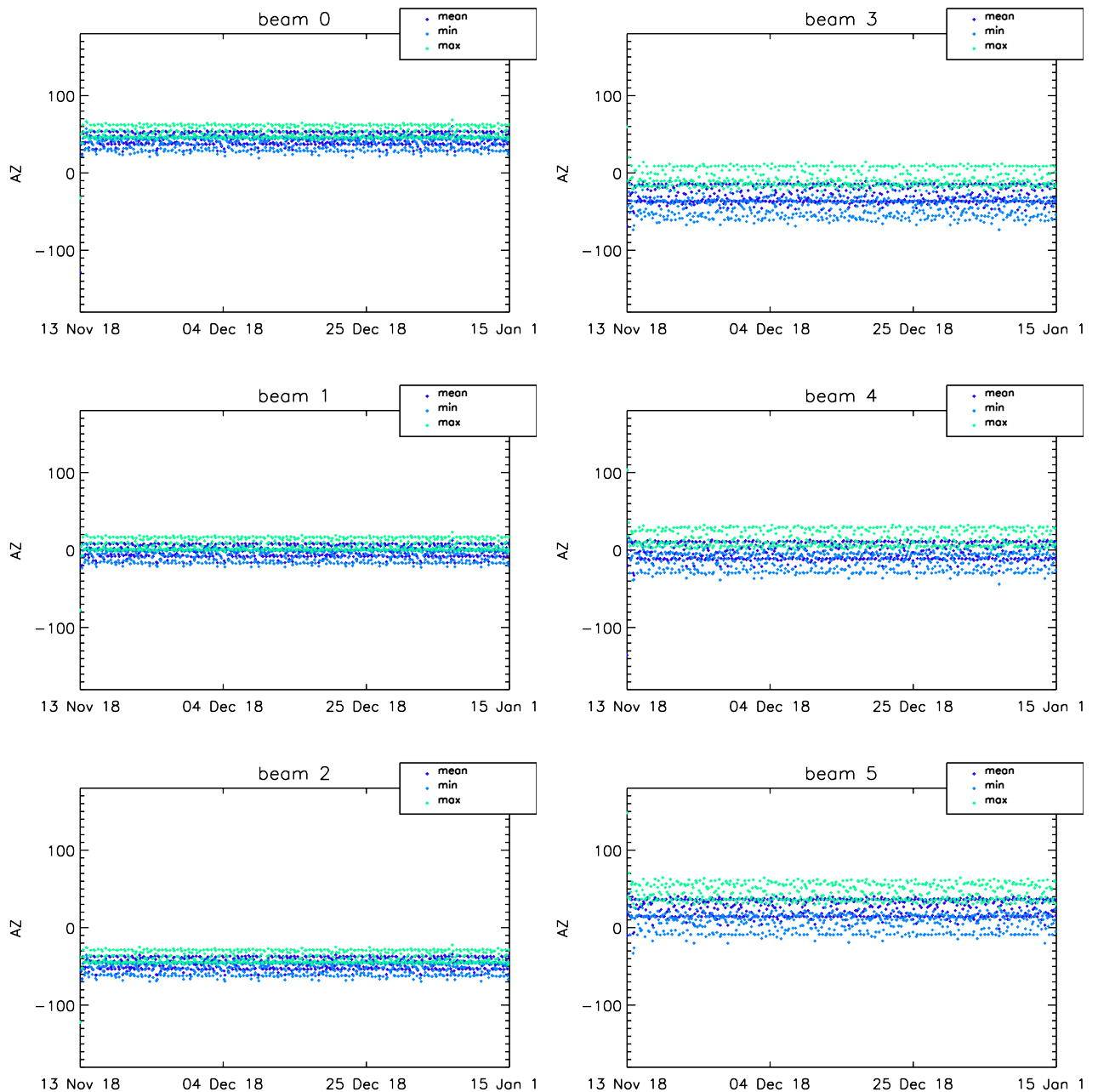
ASCAT-C Level 1 Commissioning Report


Figure 12. Azimuth angles (in degrees). The plots show three-hour average values. Data from GS1.

2.7 External calibration

External calibration of the ASCAT instruments relies on three ground based transponders. The transponders are reaching the end of their useful life and only two are available for the ASCAT-C commissioning (T1 and T3). Between 2018-11-14 and 2019-01-31, 120 transponder passes were scheduled. Of those, 98 successfully recorded data. Preliminary results are shown in Figure 13 where the ASCAT-C antenna gain values obtained from the transponder signal are shown in red (T1) and blue (T3) and compared with the gain pattern produced by the cross-calibration with ASCAT-A and B.

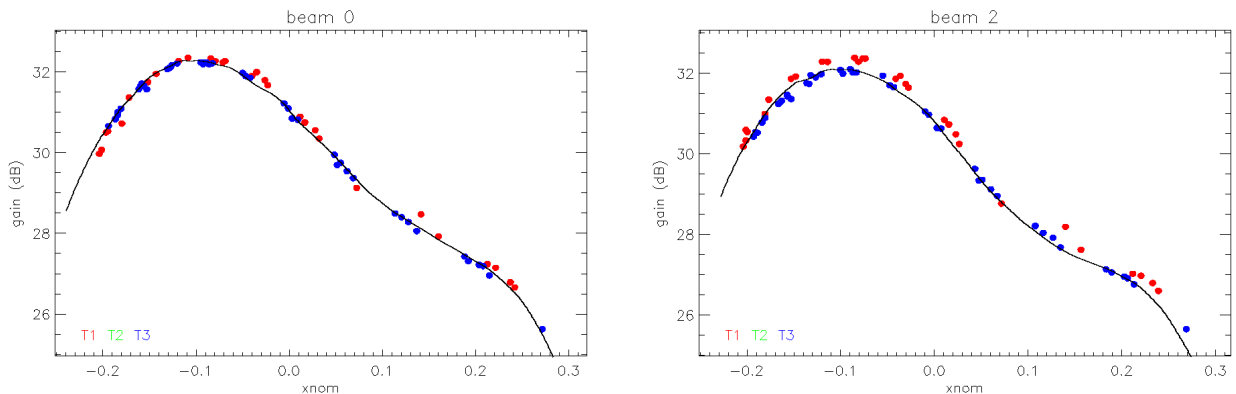


Figure 13: Antenna gain pattern. The black line shows the gain pattern from the rainforest cross-calibration. The x axis is the position of the transponder in the nominal antenna coordinate system (which is related to the elevation angle, see RD-2) Red dots are transponder gain values from T1, blue dots are transponder gains from T3.

Two issues are apparent. Firstly there are sampling problems caused by the lack of transponder T2 (i.e. regions along the x axis where there are relatively few measurements of the antenna gain). This makes it difficult to estimate the gain pattern to the required accuracy. Secondly there is a systematic deviation between the gain values provided by T1 and T3 for the aft beams (as shown in the plot for beam 2 in the above figure). For the aft beams the gain pattern from the cross-calibration and the measurements taken by T3 agree very well, but the T1 measurements show a significant offset. We have no explanation for this but it is likely related to the age and general condition of the transponders which are over a decade old and have significant reliability and maintenance problems.

These issues make the calibration process of ASCAT-C difficult and inaccurate. The decision was made to postpone the external calibration until the new transponders become operational (expected in the second half of 2019). The results will be documented in a separate report.

2.7.1 Antenna mispointing angles

The ASCAT antennas should point in specific directions. After deployment in orbit the actual antenna pointing can vary slightly from the intended nominal pointing. The pointing error (the difference between nominal and actual antenna pointing) can be estimated from the transponder data. Despite the transponder issues noted above, it is still possible to determine the antenna de-pointing angles.

The azimuth and skew de-pointing angles are determined by finding the values that make the antenna pattern from the transponder data symmetrical in the actual antenna coordinate system. The elevation de-pointing angle is determined by minimising the difference between the antenna gain values and the nominal gain pattern measured pre-launch. The angles are given below:

Table 2: Antenna mispointing angles (in radians)

beam	elevation	azimuth	skew
0	0.011	0.00045	-0.0053
1	0.017	0.00080	0.0039
2	0.015	0.0044	0.0011
3	0.020	0.0018	0.0028
4	0.009	0.0027	0.0022

5	0.005	0.0044	0.0024
----------	-------	--------	--------

The peak in each transponder signal can be geolocated and compared to the known transponder position. This gives a test of the geolocation accuracy. The table below shows the RMS difference between the estimated and true position for the original (default) and new depointing angles. The new angles improve the accuracy (particularly in the aft beams) and give consistent behaviour in all beams.

Table 3: RMS geolocation error (km)

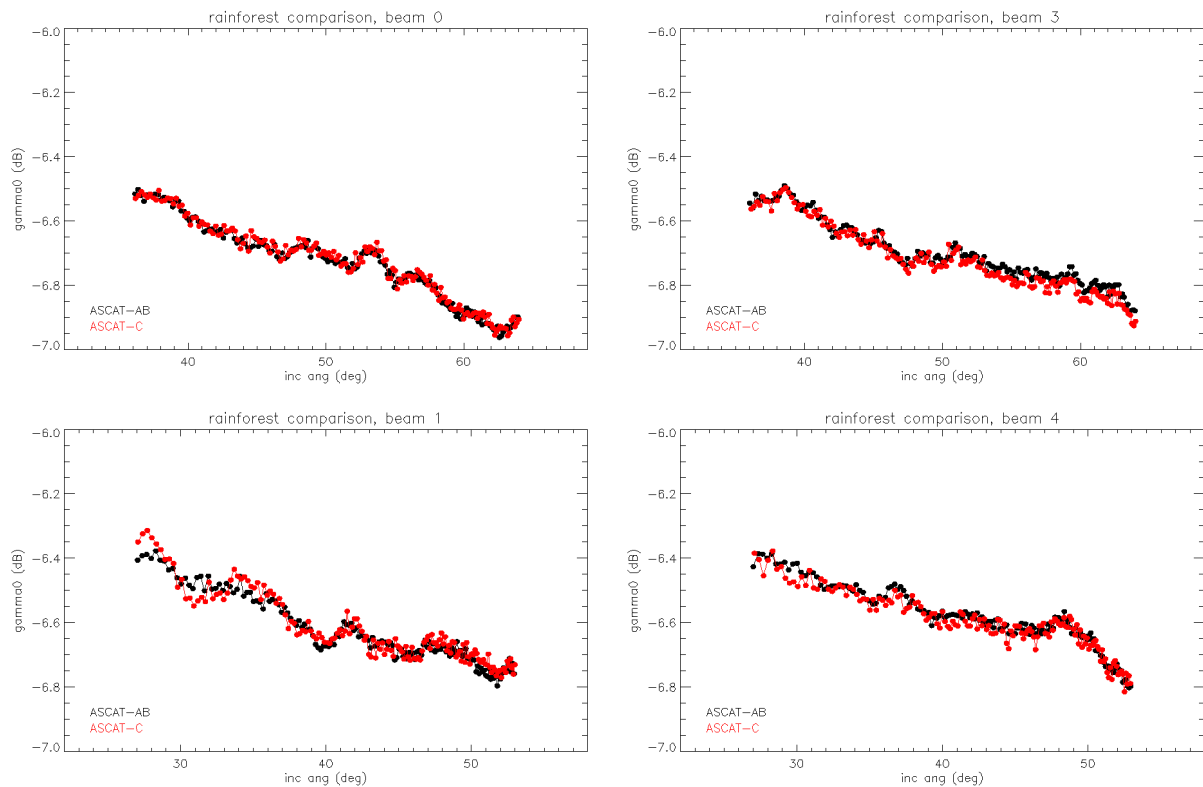
Beam	0	1	2	3	4	5
RMS (old)	2.7	2.9	8.0	4.6	4.3	7.7
RMS (new)	2.3	2.2	2.2	2.6	2.3	2.3

2.8 Improved cross-calibration

As the data provided by the transponders was judged to be unsuitable for determining an accurate gain pattern, it was decided to refine the cross-calibration by

- using the antenna depointing angles estimated from the transponder data,
- using a complete cycle (29 days) of data over the rainforest, and
- updating the cross-validation software to accurately deal with depointing angles and correct minor issues with geolocation in the aft beams.

Figure 14 shows the averaged ASCAT-A/B and ASCAT-C rainforest backscatter after the cross-calibration. The ASCAT-C backscatter matches the averaged A and B data very closely, and better than 0.1dB.



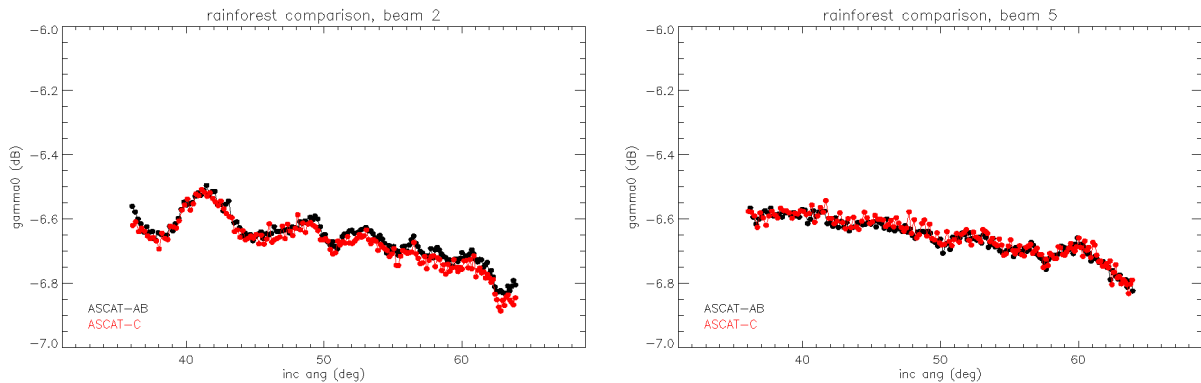
ASCAT-C Level 1 Commissioning Report


Figure 14: γ_0 patterns over the rainforest from the ASCAT-C and ASCAT-A/B cross validation data set for the time period 2018-12-14 to 2019-01-10

The gain pattern produced by this cross-calibration was introduced to GS2 on 2019-02-14 and GS1 on 2019-02-26.

2.9 Validation using natural targets

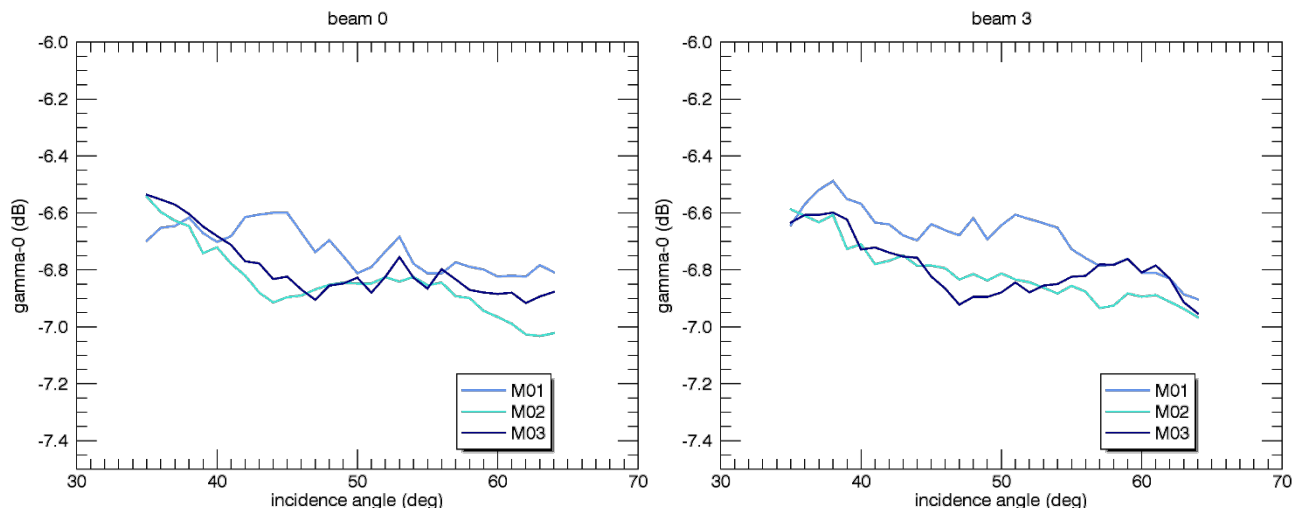
In this section we validate the refined ASCAT-C cross-calibration by examining the backscatter over a variety of natural targets and verifying that it has the expected behaviour.

The data analysed in this section was produced by GS2 during the period 2019-02-15 to 2019-02-26. The 12 days covered by this period is relatively short but given the good behaviour of the instrument and the good cross-calibration results it was considered desirable to validate the data and release products to the users as soon as possible.

2.9.1 Amazon rainforest

Backscatter over the rainforest has been studied for many years and its behaviour is well known. In particular the parameter γ_0 typically has a value of around -6.5 dB at C band.

To validate the ASCAT-C calibration we examine data from the region of Amazon rainforest bounded by the longitudes -70° and -60.5° and the latitudes -5° and 2.5° . We use data produced by the ground segment (GS2) during the period 2019-02-15 to 2019-02-25. Figure 15 shows γ_0 in each beam as a function of incidence angle and we see that the results from ASCAT-C have the expected value in all beams and are very similar to ASCAT-A and B.



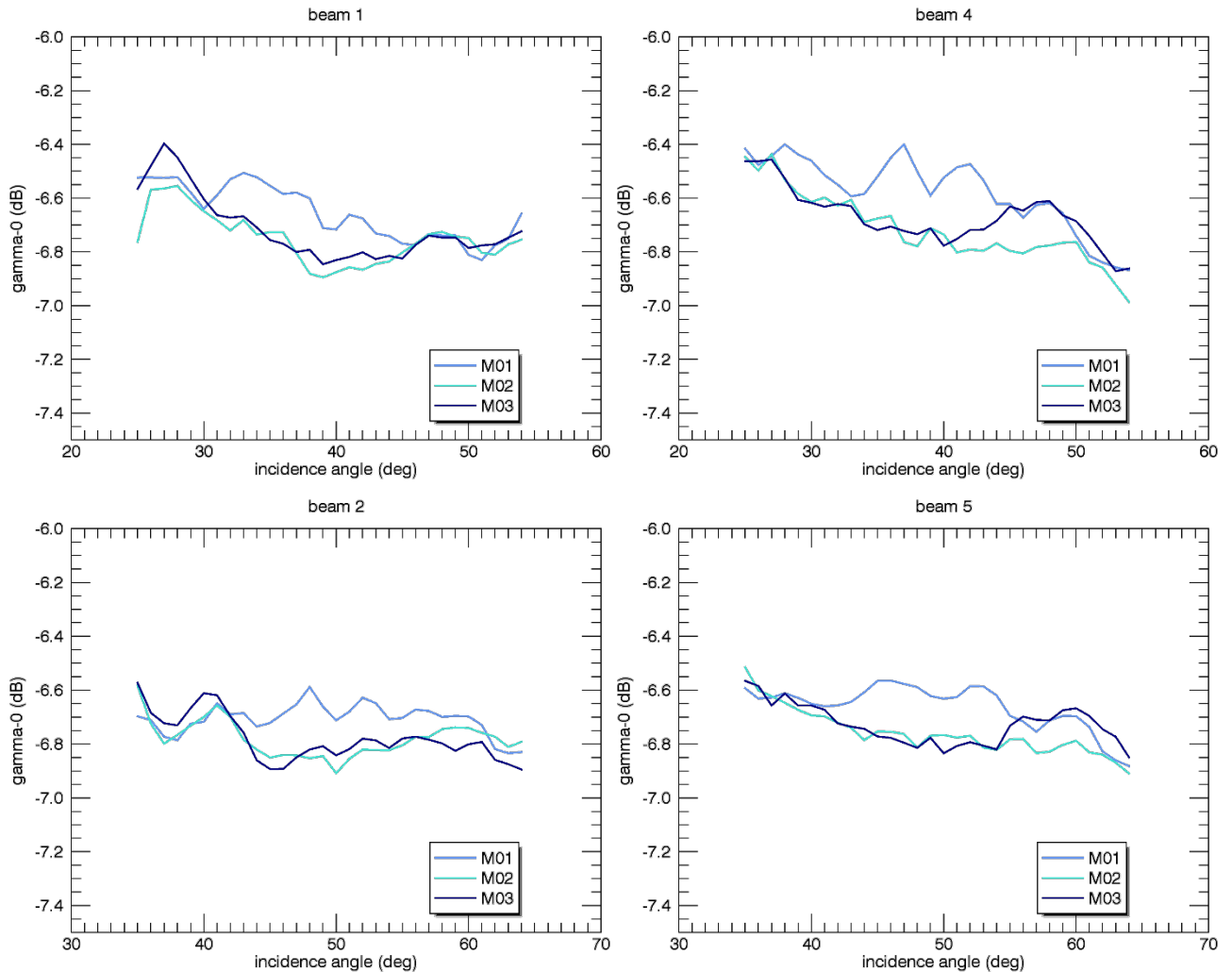
ASCAT-C Level 1 Commissioning Report


Figure 15: γ_0 as a function of incidence angle over the rainforest validation site..

This data set can also be used to investigate the relative calibration accuracy of the ASCAT-C beams. Table 4 shows the mean γ_0 in each beam and we see that the relative calibration between the different ASCAT-C beams is around 0.1 dB. The table also shows the difference of the mean γ_0 values for each beam with respect to the other ASCAT instruments, we can see that differences are typically below 0.1 dB which indicates that the cross-calibration has been successful.

Table 4: Relative calibration accuracy

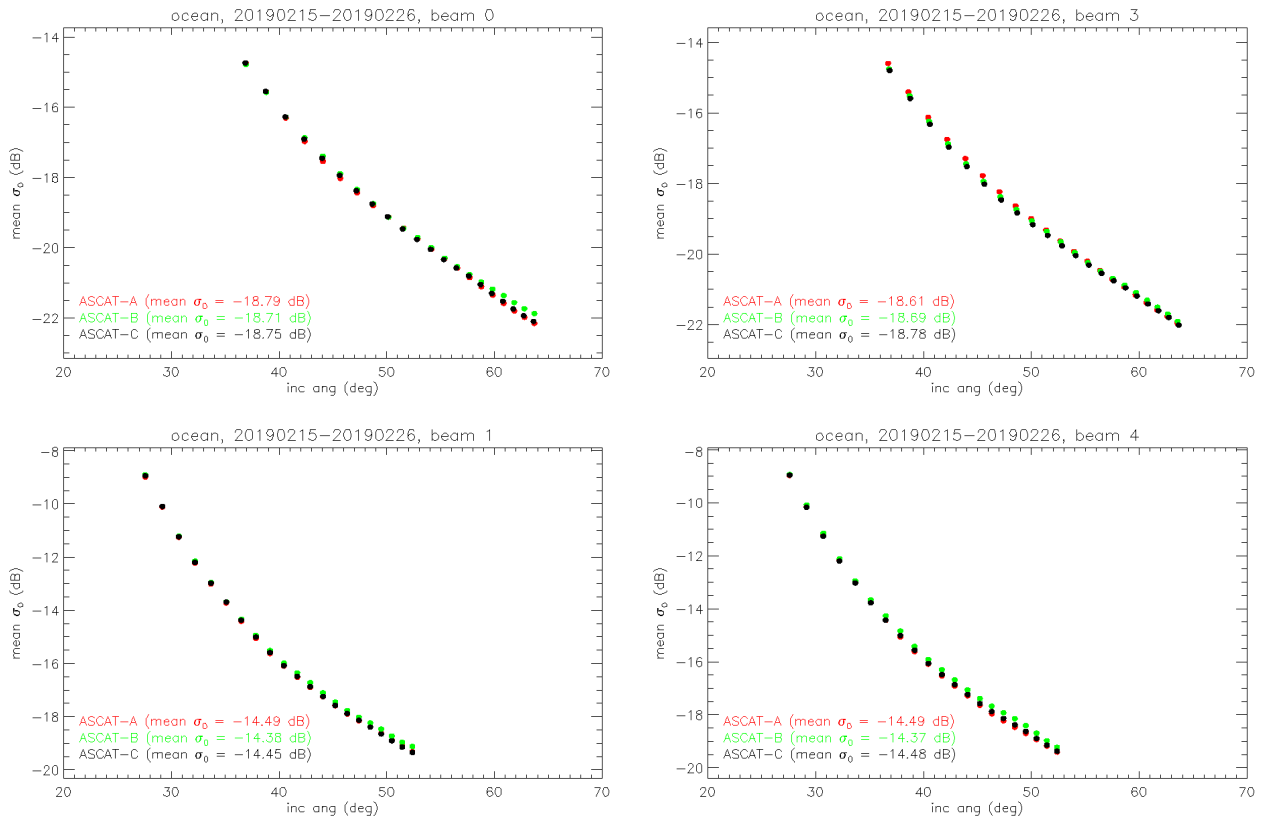
Beam	Mean γ_0 ASCAT C	Relative γ_0 ASCAT C – ASCAT B	Relative γ_0 ASCAT C – ASCAT A
0	-6.72	0.01	-0.09
1	-6.71	-0.07	-0.09
2	-6.66	0.05	-0.01
3	-6.68	0.02	0.05
4	-6.67	-0.09	0.03
5	-6.58	0.09	0.11

2.9.2 Open ocean

A variety of techniques can be used to validate an ASCAT calibration using backscatter measured from the open ocean.

The simplest approach is to look at the mean ocean backscatter. The three ASCATs have very similar viewing geometries and over a sufficiently long time period they will view the same ocean area and observe similar mean backscatter values by averaging over a large number of different wind conditions. Any systematic differences can be attributed to calibration differences.

The figure below shows the mean ocean backscatter over the period 2019-02-15 to 2019-02-26 from ASCAT-A, B and C as a function of incidence angle. The mean was calculated using backscatter from ocean between $\pm 55^\circ$ latitude and more than 200 km from land. The behaviour of all instruments is very similar. Note that in beams 2 and 3 the mean incidence angle at each of the 21 nodes across the swath shows some small variation between the instruments. This could be a real effect (caused by the pointing of the antennas) or it could be due to a small error in the depointing angles estimated from the transponder data.



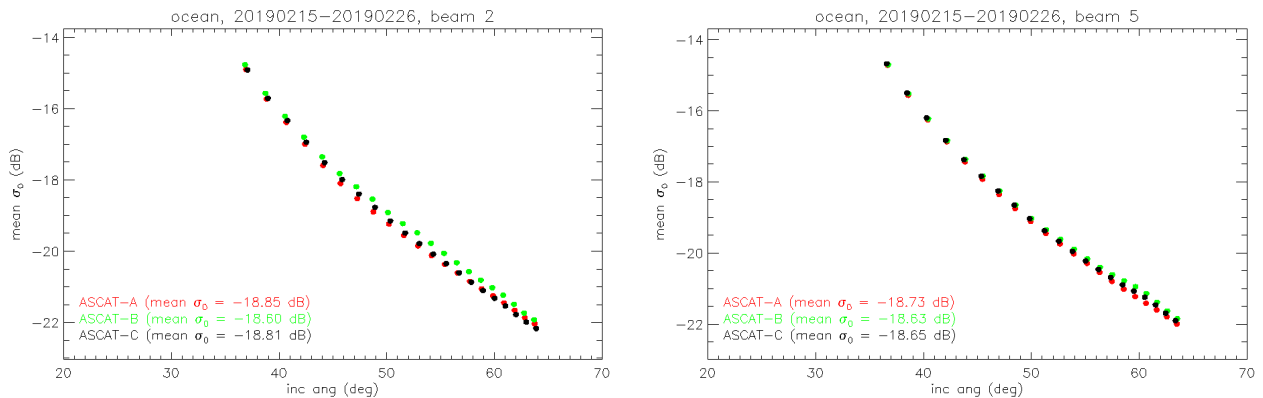
ASCAT-C Level 1 Commissioning Report


Figure 16: Mean open ocean backscatter from the three ASCATs as a function of incidence angle.

Table 5 summarises the mean difference between ASCAT-C and the other two instruments. ASCAT-C is typically within 0.1 dB of ASCAT-A and B which suggests that the cross-calibration has been successful. The largest difference is found in beam 2 where, as noted above, there is a variation in the incidence angle between the instruments which could affect the mean ocean backscatter.

Table 5: Average difference (in dB) between ASCAT-C and the other two instruments.

Beam	ASCAT-A	ASCAT-B
0	0.03	-0.06
1	0.02	-0.10
2	0.01	-0.24
3	-0.13	-0.09
4	0.03	-0.15
5	0.09	0.04

The six ASCAT beams can be grouped into three pairs - left fore and right aft, left mid and right mid, left aft and right fore. The beams in each pair view the ocean surface with azimuth angles that differ by approximately 180°. As the upwind and downwind ocean backscatter is known to be very similar the backscatter values in each beam pair should also be similar. Table 6 shows the mean ocean backscatter in each beam of ASCAT-C. Beams 0 and 5 show a difference of 0.1 dB, beams 1 and 4 show a difference of 0.03 dB and beams 2 and 3 show a difference of 0.03 dB. This suggests that the relative interbeam calibration in each pair is accurate.

Table 6: Mean open ocean backscatter in each beam of ASCAT-C

Beam	Mean σ_0
0	-18.75
1	-14.45
2	-18.81
3	-18.78
4	-14.48
5	-18.65

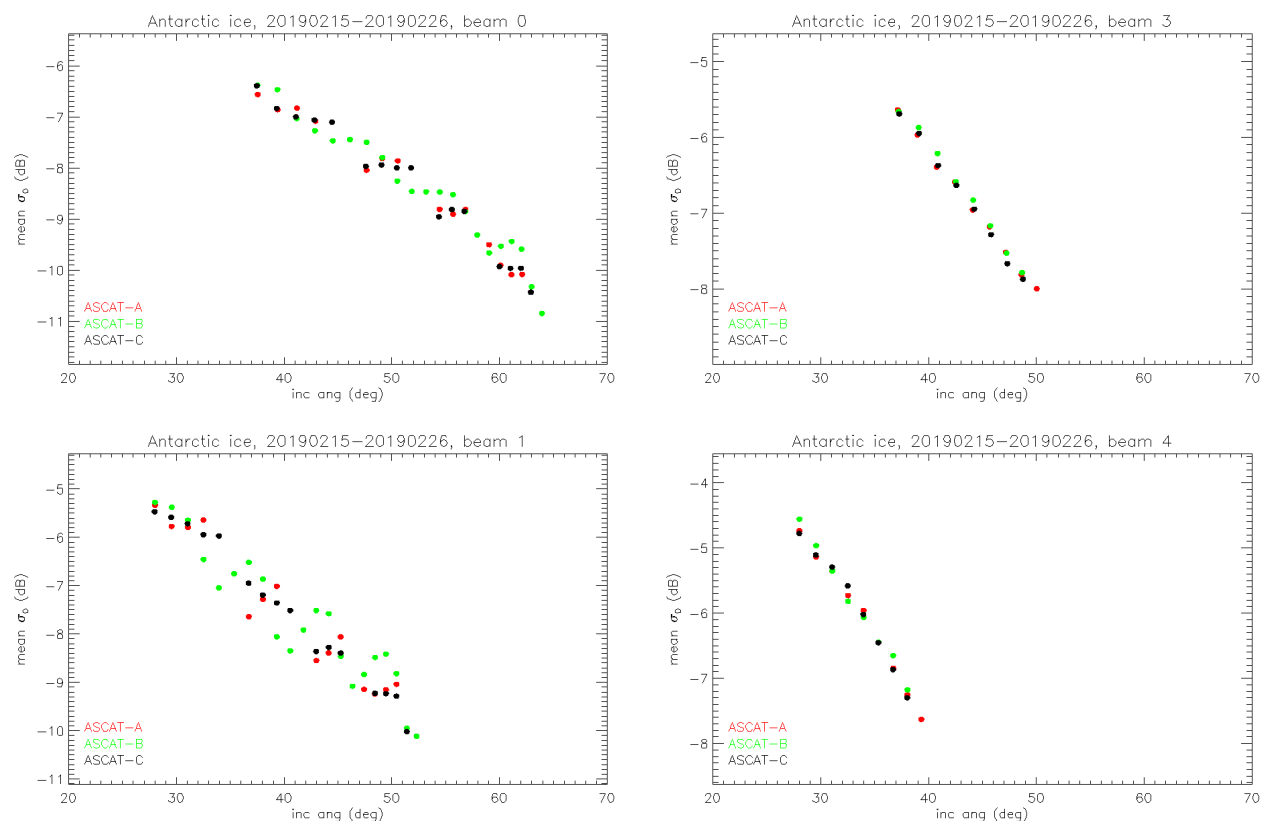
2.9.3 Antarctic ice

Environmental conditions in the Antarctic interior are stable and backscatter from this area has been examined for instrument validation and monitoring. This has advantages compared to the Amazon rainforest as polar orbiting satellites provide more data from the poles than from the equatorial region. But a number of difficulties have also been found - the backscatter from polar firn shows a large variation with incidence and azimuthal angle, the size of suitable regions showing a low spatial variability can be small, and there can be differences between the beams in the coverage of the Antarctic.

KNMI has previously examined ASCAT-A backscatter from a $2^\circ \times 2^\circ$ box centred at 77° S, 126° E and shown that it is very stable over a 7 year period with a seasonal variation of around 0.5 dB. If ASCAT-C has been correctly calibrated then we expect the mean backscatter measured in this region to be very similar to the other instruments.

Figure 17 shows the mean backscatter in this region over the period 2019-02-15 to 2019-02-26. The behaviour of all instruments is similar and there is no obvious offset between the three sets of backscatter values in each beam. This suggests that the cross-calibration is correct.

The spread of the backscatter at each node between the three instruments in this figure is larger in the left hand beams than in the right hand beams. This is likely due to the lower number of samples used to estimate the mean (around 20 samples at each incidence angle position across the swath for the left hand beams compared to around 60 or 70 in the right hand beams). Note that a more detailed validation using a larger data set will be performed following the transponder calibration in the second half of 2019.



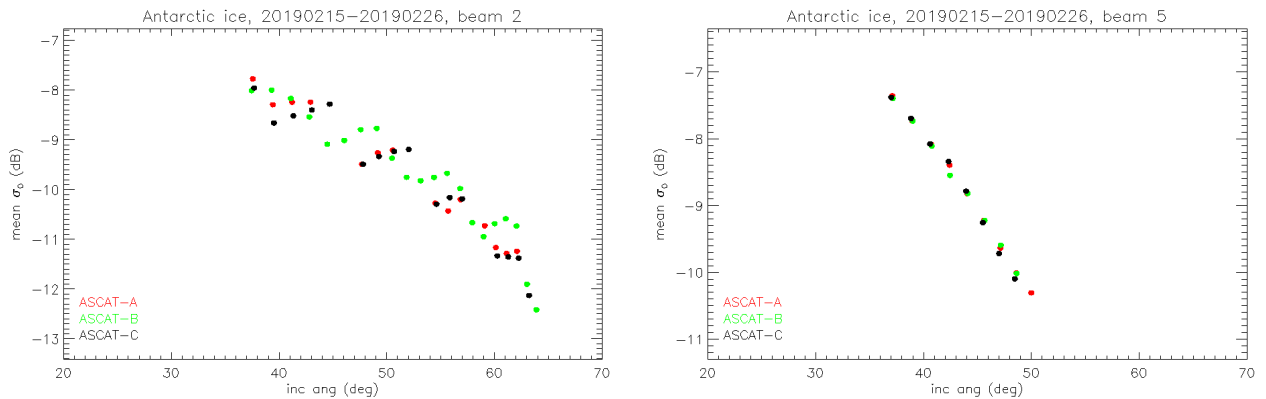
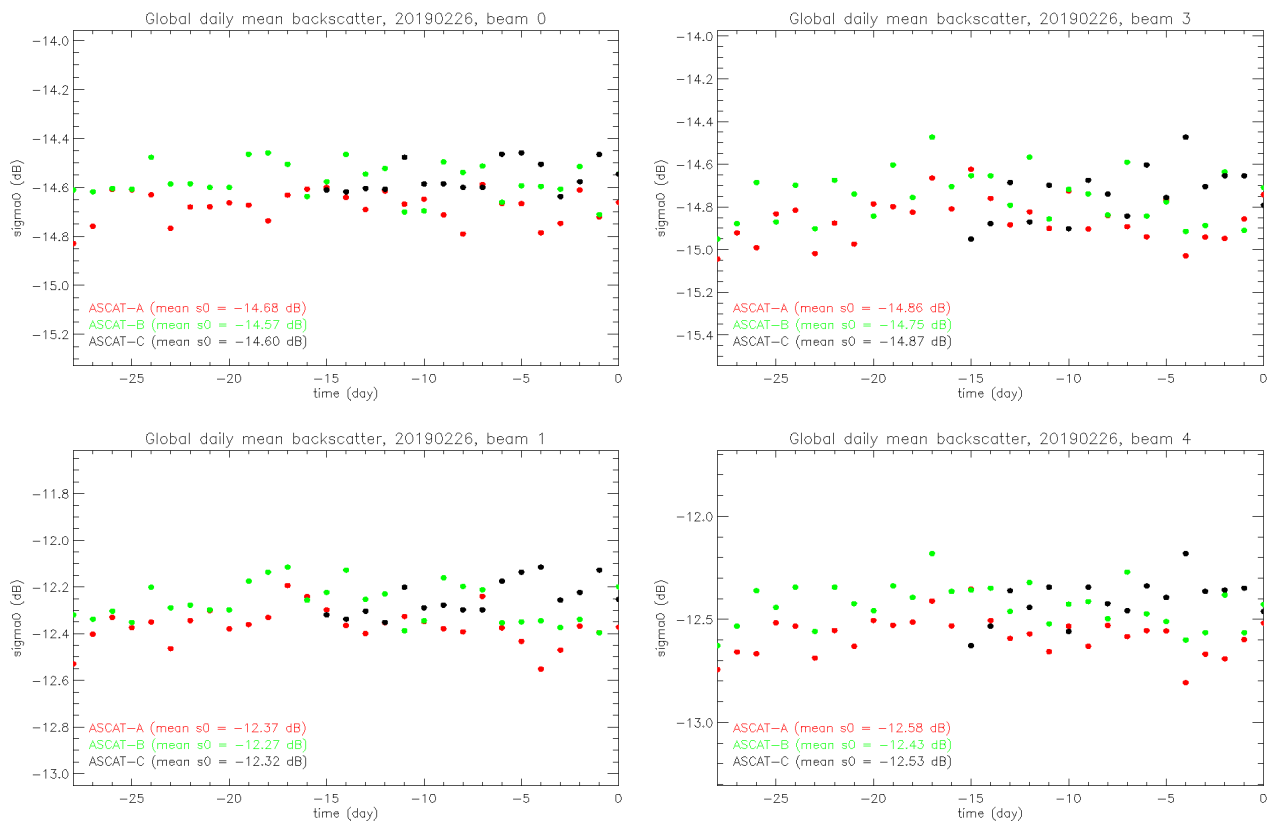
ASCAT-C Level 1 Commissioning Report


Figure 17: Mean backscatter in Antarctic ice region.

2.9.4 Global backscatter

The daily mean global backscatter from ASCAT-A and B is known to be very stable and has been used to monitor the behaviour of the instruments. If ASCAT-C has been correctly calibrated then we expect its mean backscatter values to be very similar to those of A and B. Figure 18 below shows the daily mean global backscatter from the three ASCAT instruments. The values are very similar and stable over time.



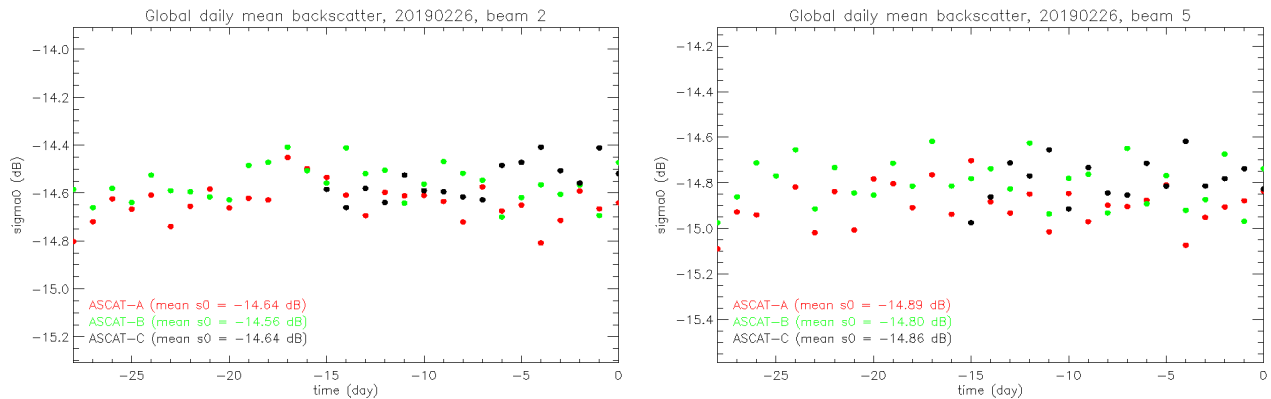
ASCAT-C Level 1 Commissioning Report


Figure 18: Mean daily global backscatter from the three ASCATs.

Table 7 summarises the differences between the ASCAT-C backscatter and the other two instruments. ASCAT-C is typically within 0.1 dB of ASCAT-A and B which suggests that the cross-calibration has been successful.

Table 7: Difference between the mean daily global backscatter of ASCAT-C and the other two instruments (dB).

Beam	ASCAT-A	ASCAT-B
0	0.07	-0.03
1	0.04	-0.06
2	0.0	-0.08
3	-0.01	-0.12
4	0.05	-0.10
5	0.03	-0.06

2.10 Accuracy of the nominal backscatter (K_p)

When the processor averages the full resolution measurements in a spatial window, it also calculates the standard deviation. The standard deviation is then used to estimate the error in the mean backscatter. This information is stored in the SZO and SZR products in the normalised form:

$$K_p = \text{estimated error in mean backscatter} / \text{mean backscatter}$$

The error in the retrieved wind speed is proportional to the error in the mean backscatter. ASCAT has a requirement that K_p over the ocean should be less than around 3%. To verify that this requirement is satisfied we extract K_p values over the ocean from SZO products for the time period from 2019-02-20 to 2019-02-25 and plot the value distribution.. The results are shown in Figure 19 and we see that the peak of the distribution of K_p is below 2% which suggests that the requirement has been met.

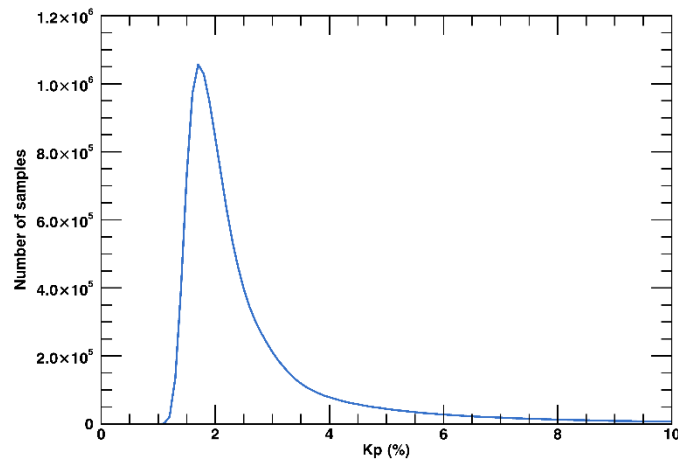


Figure 19: Kp value distribution

Figure 20 shows the percentage of values in the SZO product flagged for exceeding the Kp threshold. The drop in the percentage of flagged values at the end of January 2019 coincides with the end of the transponder calibration campaign.

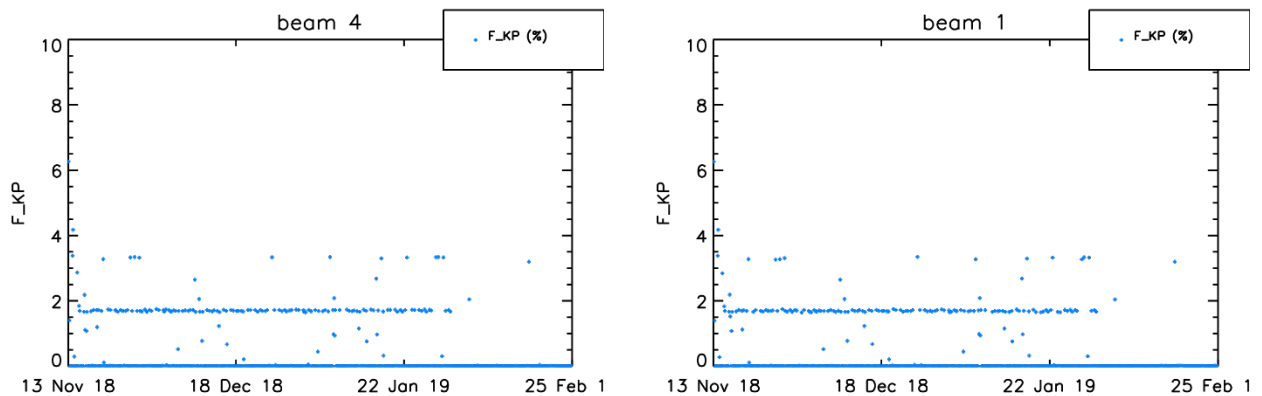


Figure 20: Time series of data flagged for exceeding the Kp threshold (F_KP). Data from GS1.

2.11 Flag validation

The quality flags produced by the processor and included in the ASCAT products were monitored and seen to behave as expected. Figure 21 tracks the F_USE flag in the SZO product. We note that F_USE is set to 2 (not usable) until mid-December 2018. This is due to an incorrect instrument ID in the INS auxiliary file. Updated INS and PRC files were provided to the GS on 13 December 2018 (see also 2.1: Internal calibration – locking of calibration constants). After the update, the F_USE flag shows the expected behaviour. The top left panel of Figure 21 shows the F_USE flag being set occasionally to 1 during the initial period of operation. This behaviour is caused by the flag tracking a possible interference from the solar array, which modifies F_USE. It is related to EUM/EP/AR/15398, and will be fixed by next ASCAT PPF release.

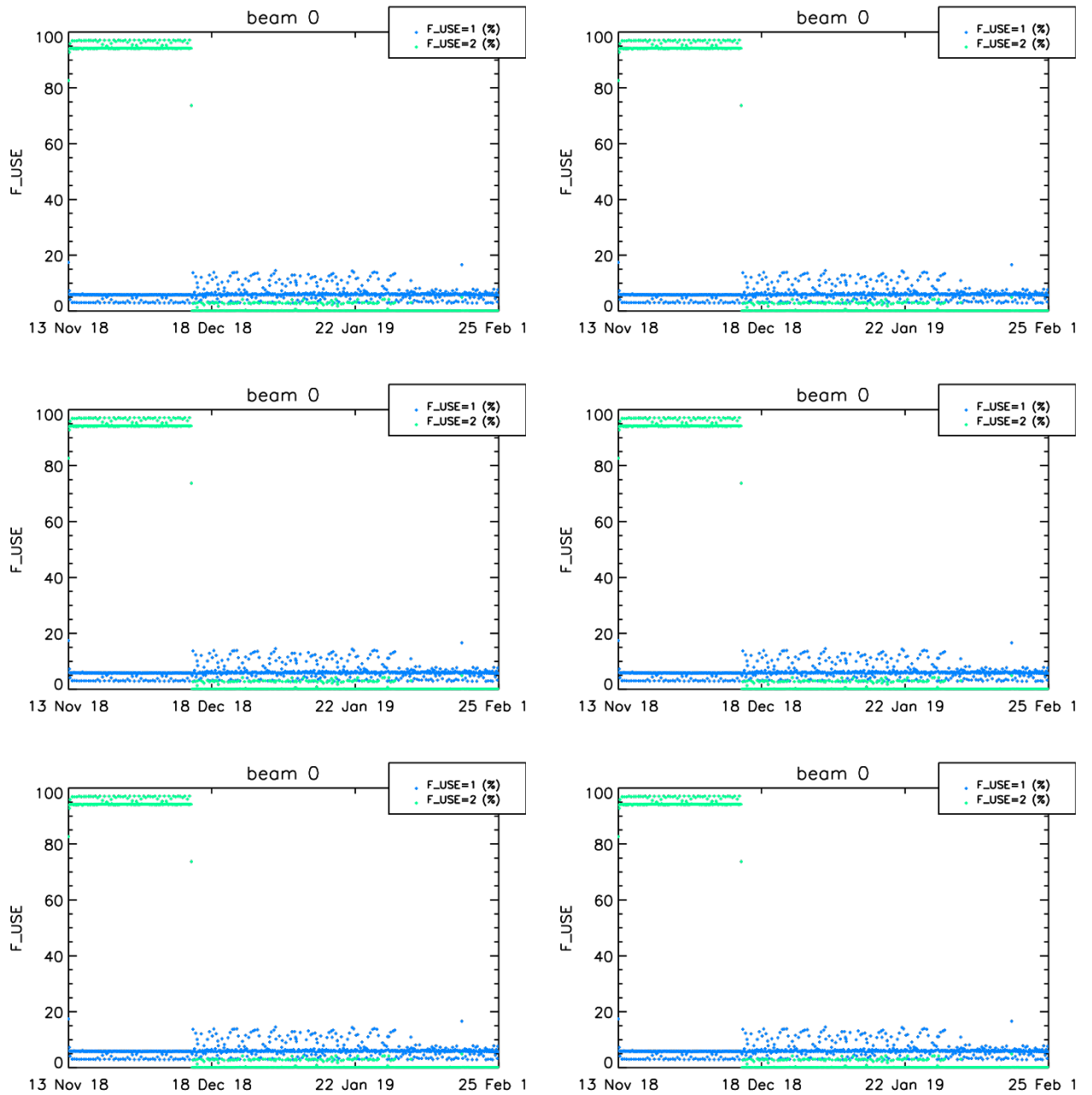
ASCAT-C Level 1 Commissioning Report

Figure 21. F_USE flag, three-hour averages. Data from GS1

3 VALIDATION BY EXTERNAL PARTNERS

The cal/val partners for the ASCAT L1b products are OSI SAF and H-SAF who cover wind and soil moisture applications. Feedback has been received from the OSI SAF (KNMI), and the H-SAF (TU-Wien). The feedback received and described below refers to the data processed with the calibration introduced to GS1 on 2019-01-22. One more calibration update has been installed after this point, this update includes a correction to the depointing angles to improve geolocation accuracy.

3.1 OSI-SAF (KNMI)

A preliminary analysis of ASCAT-C data from KNMI shows good agreement with ASCAT-A and -B, and a good quality of the wind retrieval (Figure 22).

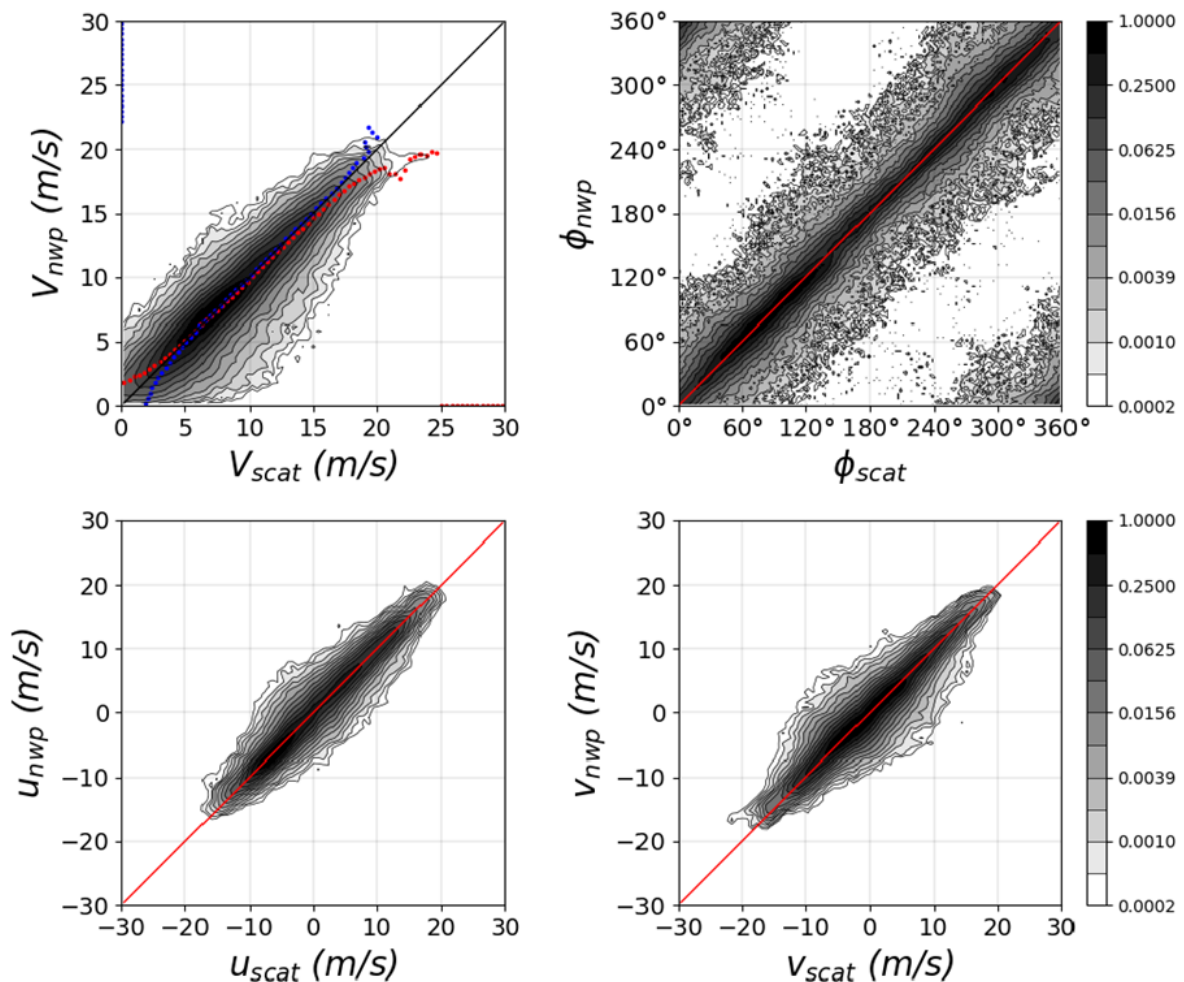


Figure 22: Wind speed (top left), wind direction (top right) and wind components (bottom) scatterplots between ASCAT-C and ECMWF collocated forecast winds for 1.5 days from 2019-01-22 to 2019-01-23. Figure courtesy of OSI SAF (KNMI).

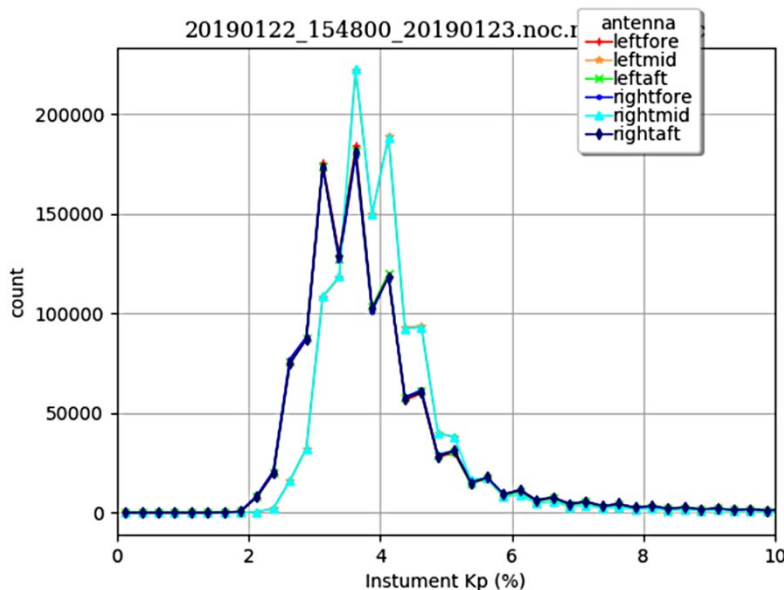


Figure 23: Kp statistics, 1.5 days from 2019-01-22 to 2019-01-23. Figure courtesy of OSI SAF (KNMI).

Figure 23 shows the distribution of Kp values per beam for 1.5 days of data beginning on 2019-01-22. The OSI SAF (KNMI) produces SZO-based winds and SZF-based coastal winds routinely from ASCAT-C and quality monitoring statistics can be accessed through www.knmi.nl/scatterometer.

3.2 H-SAF (TU-Wien)

A preliminary qualitative analysis of the soil moisture products produced by the H SAF processor shows good agreement between ASCAT-A (not shown here), ASCAT-B and -C in the distribution of soil moisture patterns (Figure 24) and the spatial distribution of the retrieval error (Figure 25).

Specific feedback on the quality of the soil moisture data is covered in the ASCAT-B soil moisture validation report and is not included here.

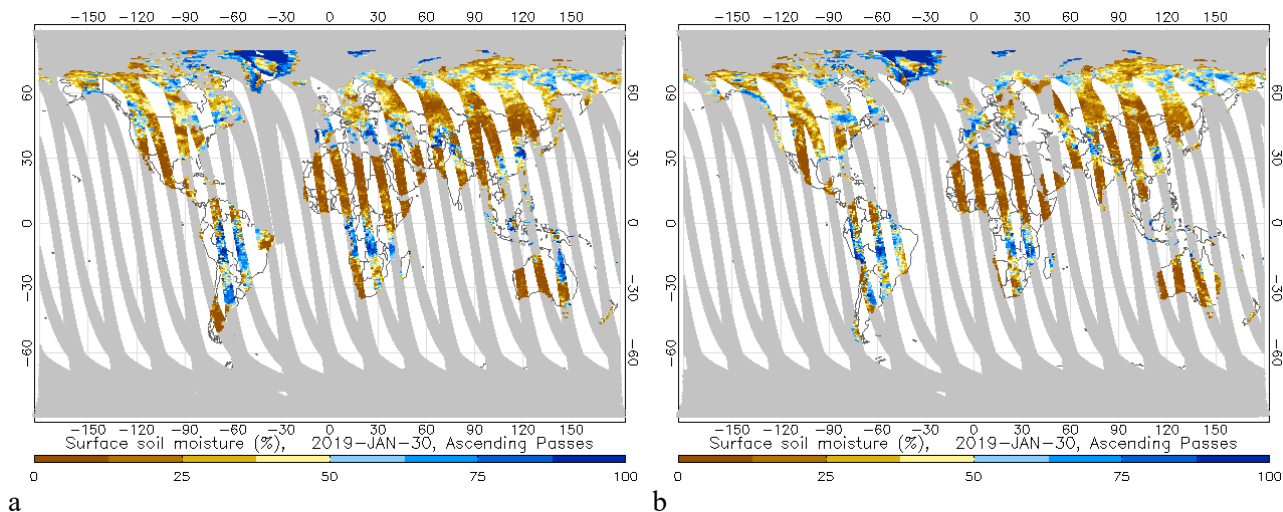


Figure 24: Surface soil moisture on 2019-01-30 for a) Metop-B, b) Metop C, ascending passes.

ASCAT-C Level 1 Commissioning Report

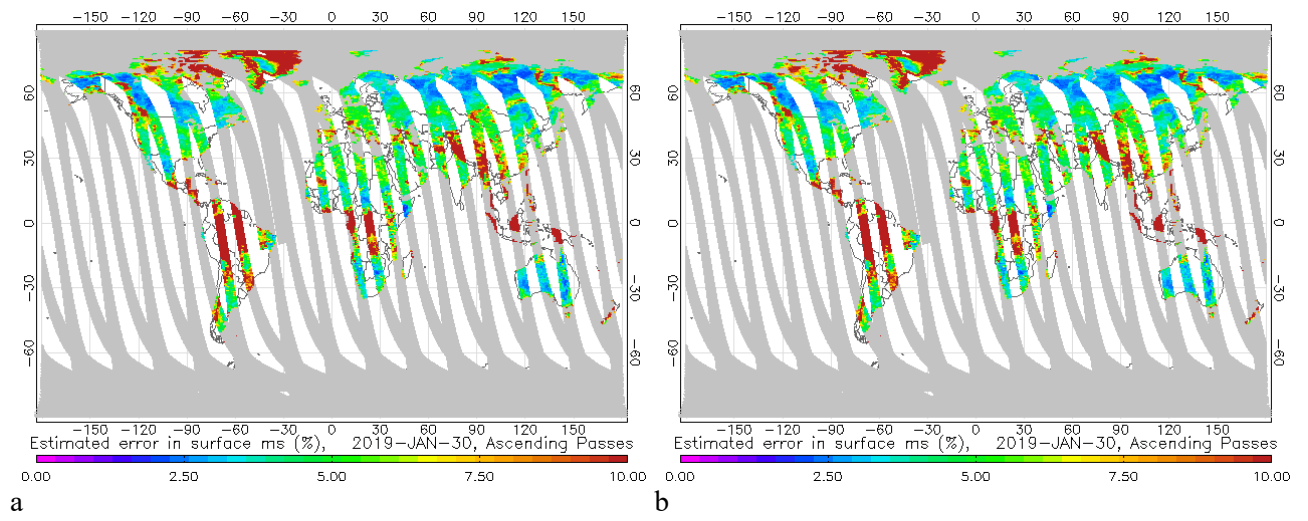


Figure 25: Surface soil moisture error on 2019-01-30 for a) Metop-B, b) Metop C, ascending passes.

4 SUMMARY AND CONCLUSIONS

ASCAT-C was switched on shortly after the launch of Metop-C. During the SIOV phase the instrument manufacturer reported two minor anomalies - larger than expected transmit power in the right mid beam and larger than expected reflected power in the right aft beam. Investigations are ongoing but both anomalies are small and are expected to have negligible impact on the instrument performance.

The activities described in the ASCAT-C cal/val plan were performed, namely

- an initial cross-calibration with ASCAT-A and B,
- external calibration using transponder signals,
- validation of the level 1b data using a number of natural targets,
- monitoring of the science and telemetry data,
- analysis of the level 2 data from the OSI-SAF and H-SAF.

The initial cross-calibration with ASCAT-A and B was based on data from the Amazon rainforest from the period 2018-12-14 to 2019-01-07. The results in the mid and aft beams were good but small discrepancies of around 0.2 dB were noted in the fore beams. This calibration was introduced into GS1 on 2019-01-22.

Only two transponders (T1 and T3) were available for ASCAT-C external calibration and the data set collected between 2018-11-14 and 2019-01-31 showed several problems: poor sampling of the gain patterns (due to the lack of T2) and significant differences between the data from T1 and T3 in the aft beams (reason unknown). The collected data was considered unsuitable for an accurate calibration but the antenna pointing could be accurately estimated and improves the RMS ASCAT-C geolocation error from 8 km to around 2 km. The external calibration will be re-attempted after the new transponders are installed in the second half of 2019.

The cross-calibration was then improved by making use of the new pointing angles, a longer rainforest data set, and upgraded cross-calibration algorithms and software. The results showed a very good alignment of ASCAT-A, B and C data and the improved cross calibration was introduced into the GS1 on 2019-02-26.

Validation of the ASCAT-C data was then performed using a variety of natural targets (Amazon rainforest, open ocean, Antarctic ice and global backscatter). Although the data set was limited to a few weeks the results were consistent and showed that the backscatter from all three ASCAT instruments is similar to around 0.1 dB and that the relative interbeam calibration accuracy of ASCAT-C is around 0.1 dB (For comparison: an error of 0.1 dB in the backscatter is usually assumed to introduce an error of 0.1 ms⁻¹ in the retrieved ocean wind speed).

Monitoring of the telemetry, science data and flagging has shown that the ASCAT-C behaves very well, and is very stable. The only minor point to note is that the power-gain product (calculated from internal calibration data and used in the conversion of instrument measurements into normalised radar cross section) took longer than expected to stabilise.

Analysis performed by the external partners (KNMI, TU-Wien) indicates that the data from ASCAT-C is of high quality and gives results that are very similar to the data from ASCAT-A and B.

Based on the results presented in this document and feedback from the external partners we conclude ASCAT-C has been successfully cross-calibrated with ASCAT-A and B and shows no issues that prevent its data from being released for operational use.

Note that three new transponders will be installed in the second half of 2019 which will allow the external calibration of ASCAT-C to be completed.

ASCAT-C Level 1 Commissioning Report**APPENDIX A GROUND SEGMENT CONFIGURATION CHANGES**

PPF tuning and validation has been done on GS2 / GS1. GS3 has been kept aligned but has not been used or monitored. The following is a list of updates of the ASCAT Level 1 PPF in G3/2/1 since launch.

Files	svn release	Installed on GS2	Installed on GS1	SWET	Comment
PRC, XCL	20.0.0	2018-12-13	2018-12-13	EPS_SWET_2453	Ccal locking, corrected instrument ID
INS	21.0.0	2019-01-16	2018-01-22	EPS_SWET_2467	Updated gain patterns, 1 st cross-calibration with ASCAT A/B
INS, XCL	22.1.0	2019-02-14	2019-02-26	EPS_SWET_2490	Updated pointing based on transponder data, refined cross-calibration with ASCAT A/B

APPENDIX B INSTRUMENT TELEMETRY
B.1 Temperatures

The following plots show time series of SFE and ANT temperatures from HKTM data. Thresholds applied in the Level 1 processor are $-27\text{ }^{\circ}\text{C}$ and $56\text{ }^{\circ}\text{C}$ for the SFE temperatures (Figure 26).

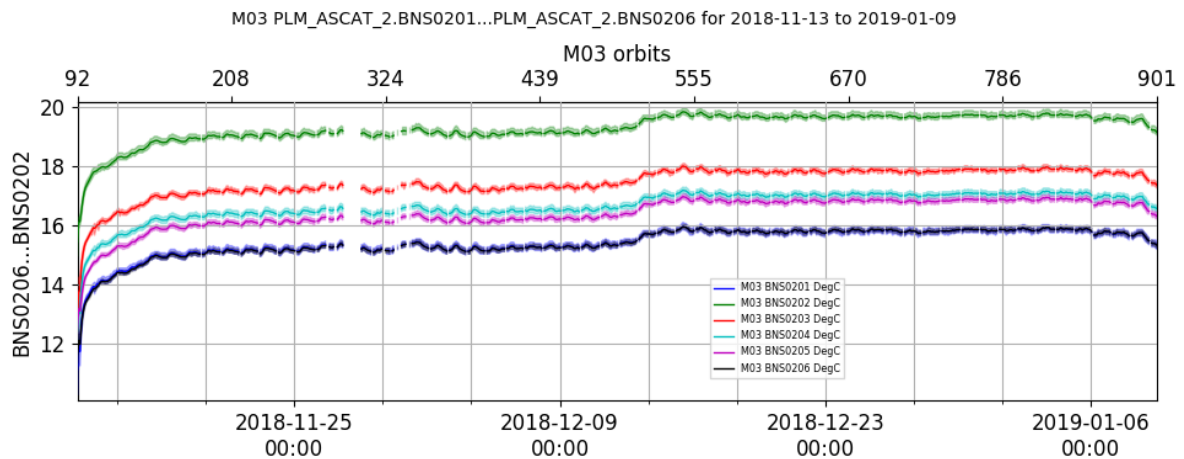


Figure 26: SFE temperatures 1-6

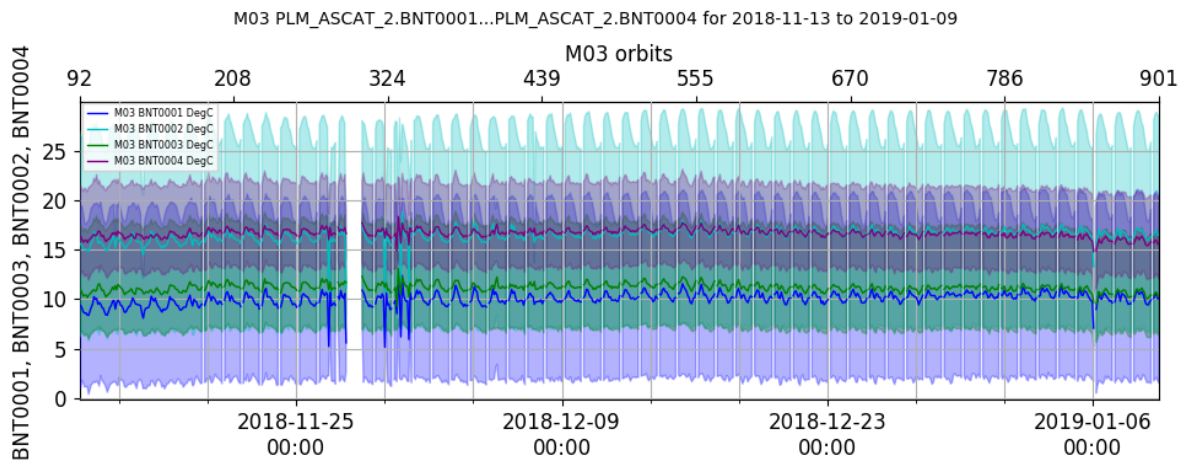


Figure 27: Antenna temperatures 1-4

The valid temperature range for the parameters show in Figure 27 is between $-17\text{ }^{\circ}\text{C}$ and $62\text{ }^{\circ}\text{C}$.

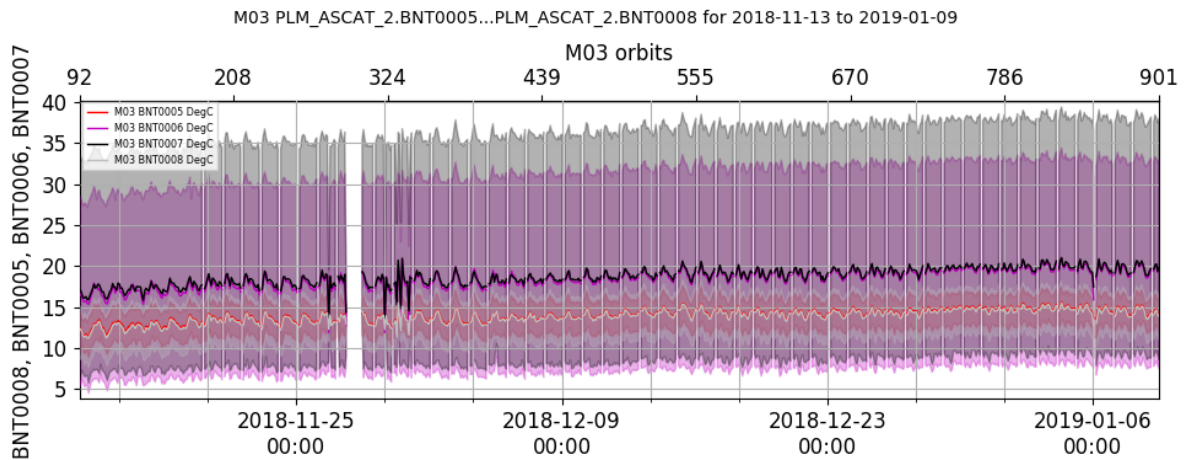


Figure 28: Antenna temperatures 5-8

The valid temperature range for the parameters show in Figure 28 is between $-17\text{ }^{\circ}\text{C}$ and $57\text{ }^{\circ}\text{C}$.

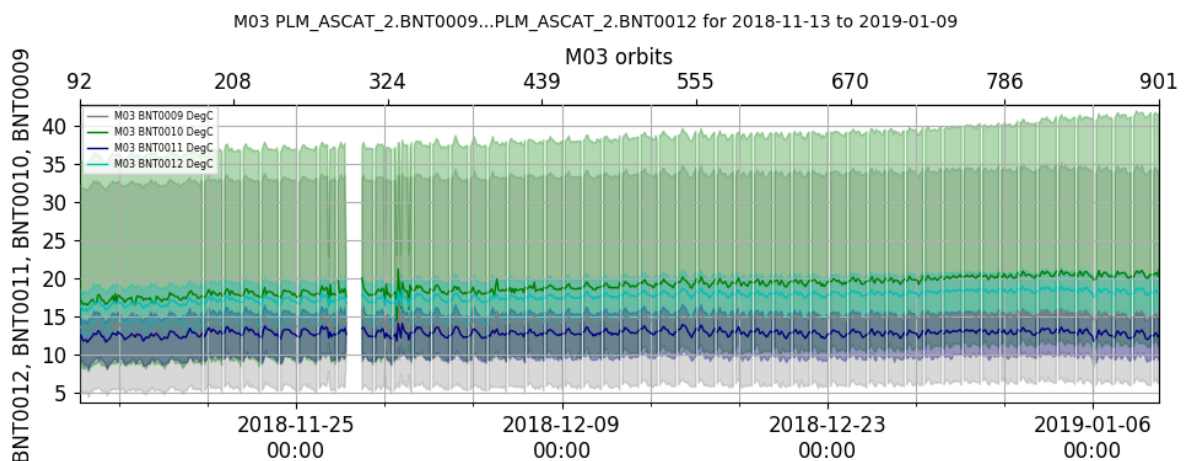


Figure 29: Antenna temperatures 9-12

The valid temperature range for the parameters show in Figure 29 is between $-17\text{ }^{\circ}\text{C}$ and $62\text{ }^{\circ}\text{C}$. All temperature values are within the limits.

B.2 Equipment voltages

The following plots show time series of equipment voltages from HKTm telemetry. The lower / upper thresholds applied in the Level 1 processor are 21.0 V and 37.5 V, respectively, for DPU / RFU / SFE and HPA voltages. All values are within those limits.

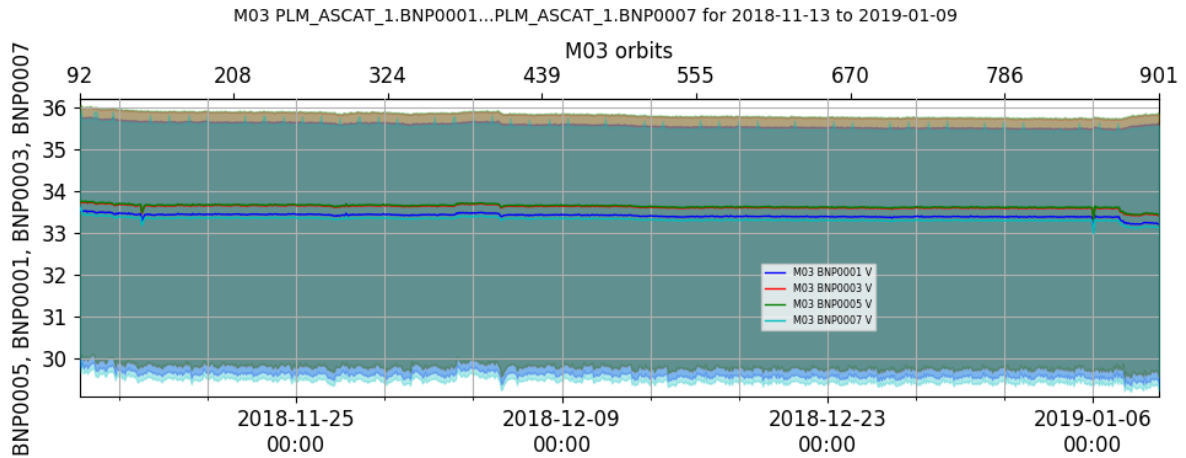
ASCAT-C Level 1 Commissioning Report


Figure 30: Voltages – DPU (BNP0001), RFU (BNP0005), SFE (BNP0003) and HPA (BNP0007)

B.3 Equipment powers

Time series of equipment powers from HKTM telemetry. The valid range for DPU powers is between 7.65 W and 32.8 W (Figure 31), for RFU powers between 17.18 W and 26.51 W (Figure 31), and for SFE between 10.93 W and 21.24 W (Figure 32). All values are nominal.

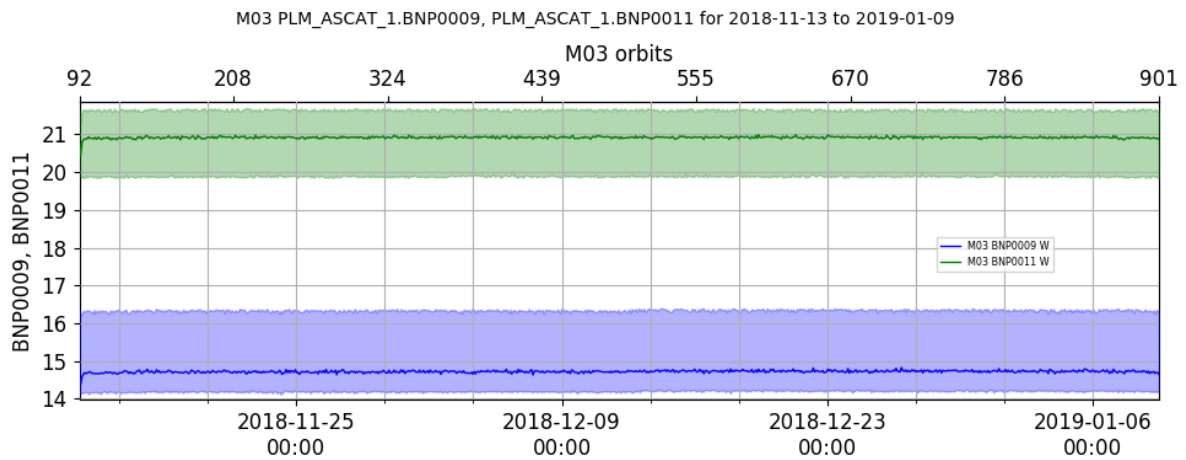


Figure 31: Powers – DPU (BNP0009) and RFU (BNP0011)

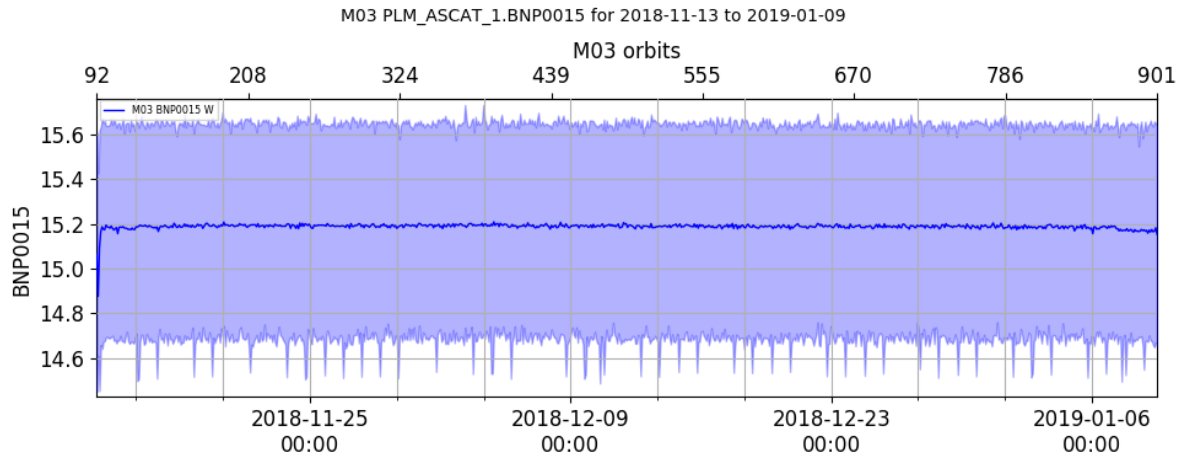
ASCAT-C Level 1 Commissioning Report


Figure 32: SFE powers

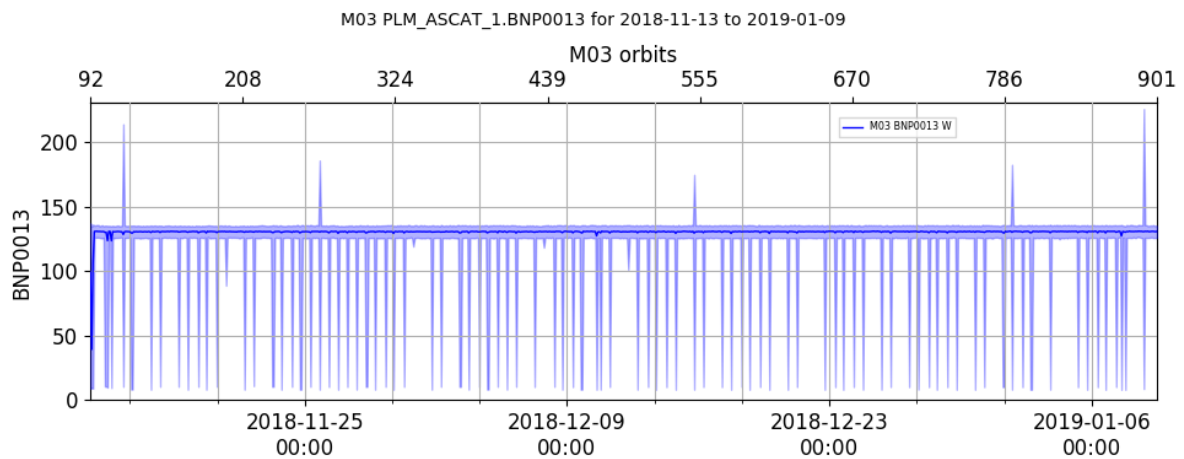


Figure 33: HPA power, ASCAT-C

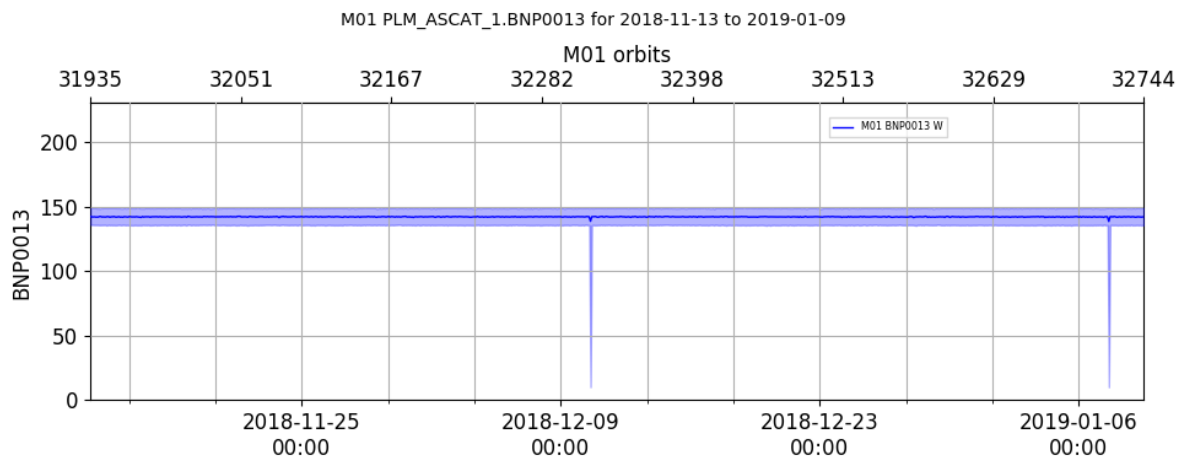


Figure 34: HPA power, ASCAT-B

Figure 34 shows the HPA power. The valid range is between 3.23 W and 206.04 W.

B.4 Equipment temperatures

The plots below show time series of equipment temperatures from HKTM telemetry. The valid temperature range for all parameters show below (Figure 35 and Figure 36) is between -17 °C and 54 °C. All values are within the limits.

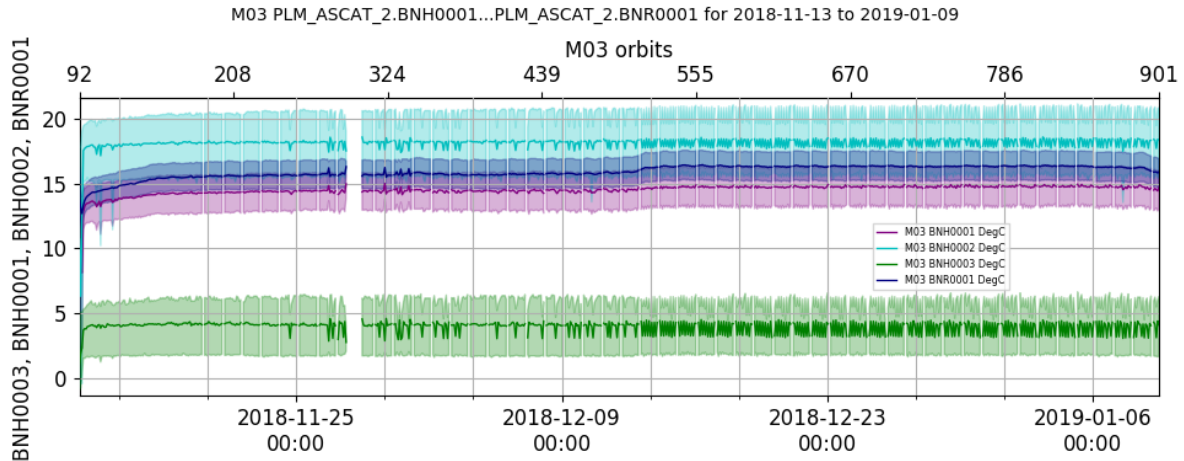


Figure 35: T_{SSPA1A} (BNH0002), T_{SSPA2A} (BNH0003), T_{EPCA} (BNH0001), T_{RFUA} (BNR0001)

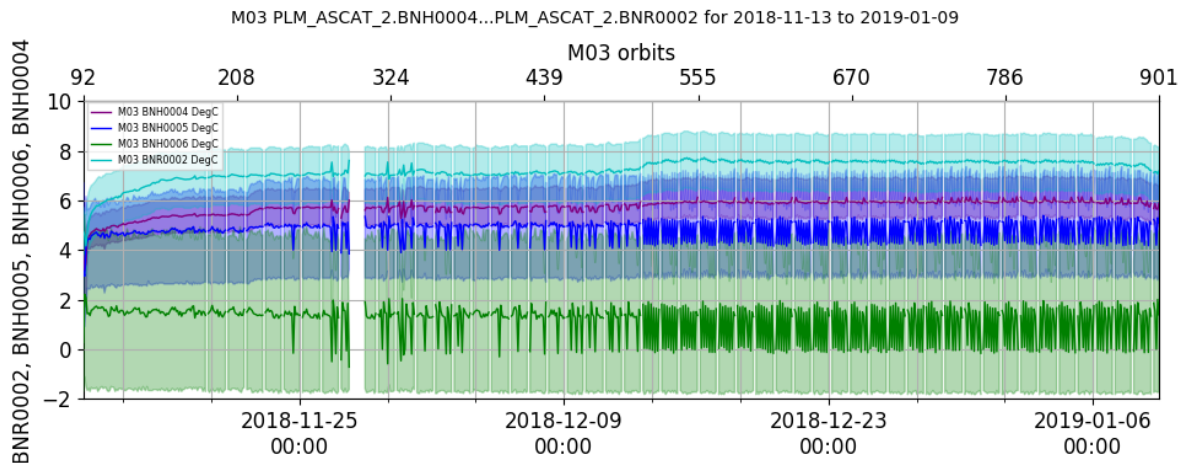


Figure 36: T_{SSPA1B} (BNH0005), T_{SSPA2B} (BNH0006), T_{EPCB} (BNH0004), T_{RFUB} (BNR0002)

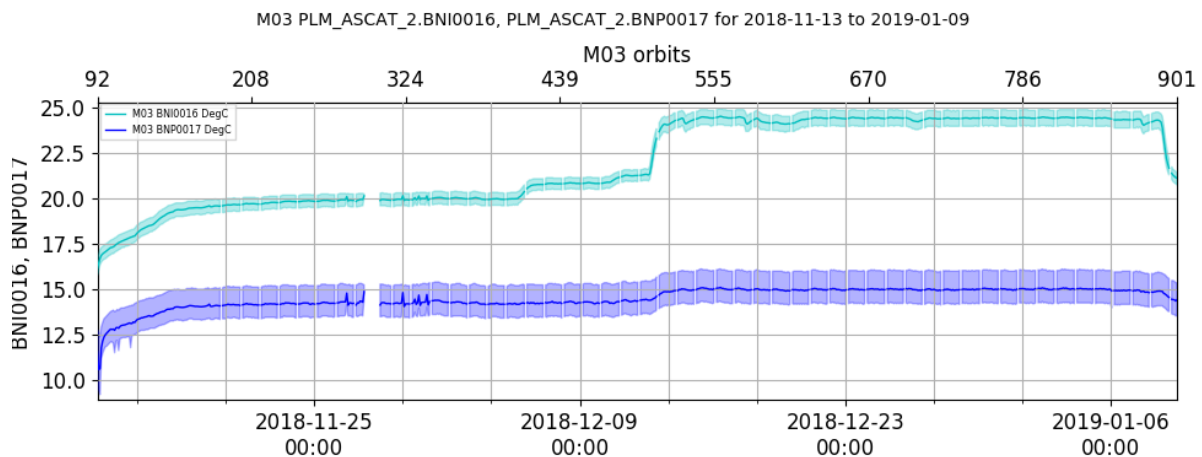


Figure 37: T_PDU (BNP0017, T_ICU (BNI0016)

The valid temperature range for the PDU is between $-27\text{ }^{\circ}\text{C}$ and $56\text{ }^{\circ}\text{C}$ and for the ICU between $-32\text{ }^{\circ}\text{C}$ and $59\text{ }^{\circ}\text{C}$ (Figure 37). All values are nominal.

Figure 36 and Figure 37 show the impact of other instruments on the temperature – the most prominent effect can be seen in the ICU temperatures and is due to IASI switch-on in mid-December 2018 and temporary switch-off in mid-January 2019.

B.5 ADC Voltages, gain and offsets

The following plots show time series of ADC voltages, gain and offsets from HKTM telemetry.

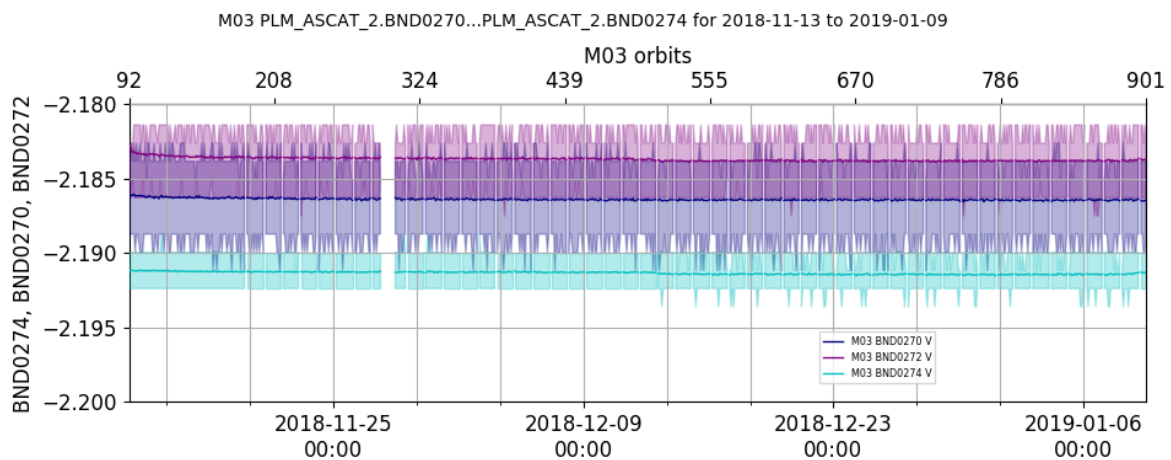


Figure 38: fwd/cal ADC VR1 (BND0270), reflected ADC VR1 (BND0272), main ADC VR1 (BND0274)

The valid range for the voltages shown in Figure 38 is between -2.2313 V and -2.1438 V . All measurements are within the limits.

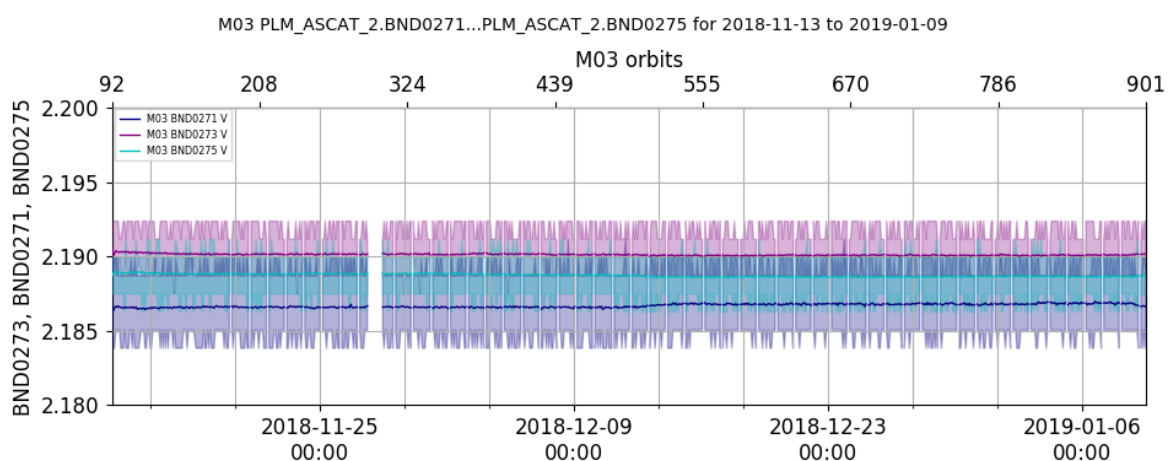


Figure 39: fwd/cal ADC VR2 (BND0271), reflected ADC VR2 (BND0273), main ADC VR2 (BND0275)

The valid range for the voltages shown in Figure 39 is between 2.1438 V and 2.2313 V . All measurements are within the limits.

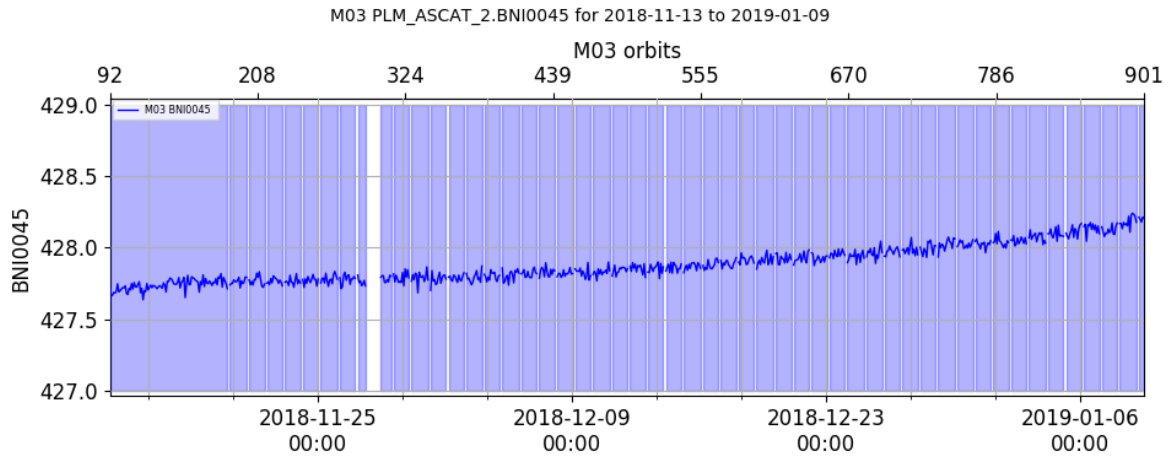
ASCAT-C Level 1 Commissioning Report


Figure 40: Offset_AD (BNI0045)

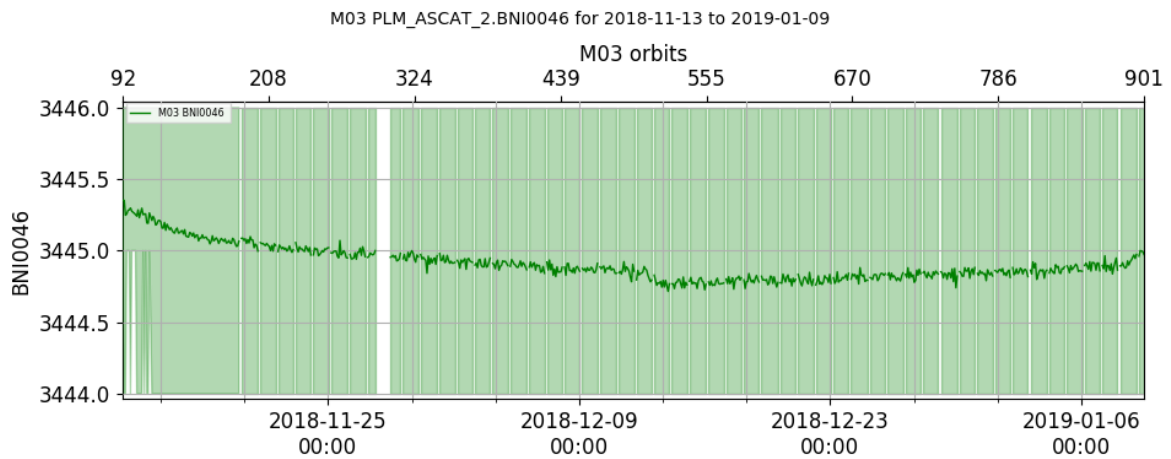


Figure 41: Gain_AD (BNI0046)

The thresholds defined in the L1 processor for the Offset_AD are 412 and 454 (Figure 40), and for Gain_AD 3415 and 3477 (Figure 41). All values are within the respective limits.